Chapter

7

Components of Optical Instruments

Instruments for ultraviolet and infrared spectroscopy have enough features in common with those designed for the visible region that they are commonly called optical instruments despite the fact that the human eye is sensitive to neither ultraviolet nor infrared wavelengths. In this chapter, we consider the function, the requirements, and the behavior of the components of instruments for optical spectroscopy employing all three types of radiation. Instruments for spectroscopic studies in regions more energetic than the ultraviolet and less energetic than the infrared have characteristics that differ substantially from optical instruments and are considered separately in Chapters 12 and 19.

7A GENERAL DESIGNS OF OPTICAL INSTRUMENTS

Optical spectroscopic methods are based upon six phenomena: (1) absorption, (2) fluorescence, (3) phosphorescence, (4) scattering, (5) emission, and (6) chemiluminescence. While the instruments for measuring each differ somewhat in configuration, most of their basic components are remarkably similar. Furthermore, the required properties of these components are the same regardless of whether they are applied to the ultraviolet, visible, or infrared portion of the spectrum.[1]

Typical spectroscopic instruments contain five components, including: (1) a stable source of radiant energy; (2) a transparent container for holding the sample; (3) a device that isolates a restricted region of the spectrum for measurement[2]; (4) a radiation detector, which converts radiant energy to a usable signal (usually electrical); and (5) a signal processor and readout, which displays the transduced signal on a meter scale, an oscilloscope face, a digital meter, or a recorder chart. Figure 7-1 illustrates the three ways in which these components are configured in order to carry out the six types of spectroscopic measurements mentioned earlier. As can be seen in the figure, components (3), (4), and (5) are arranged in the same way for each type of measurement.

[1] For a more complete discussion of the components of optical instruments, see R. P. Bauman, *Absorption Spectroscopy,* Chapters 2 and 3. New York: Wiley, 1962; E. J. Meehan, in *Treatise on Analytical Chemistry,* P. J. Elving, E. J. Meehan, and I. M. Kolthoff, Eds., Part I, Vol. 7, Chapter 3. New York: Wiley, 1981; J. D. Ingle Jr. and S. R. Crouch, *Spectrochemical Analysis,* Chapters 3 and 4. Englewood Cliffs, NJ: Prentice Hall, 1988.

[2] Fourier transform instruments, which are discussed in Section 7I-3, require no wavelength selecting device but instead use a frequency modulator that provides spectral data in a form that can be interpreted by a mathematical technique called a Fourier transformation.

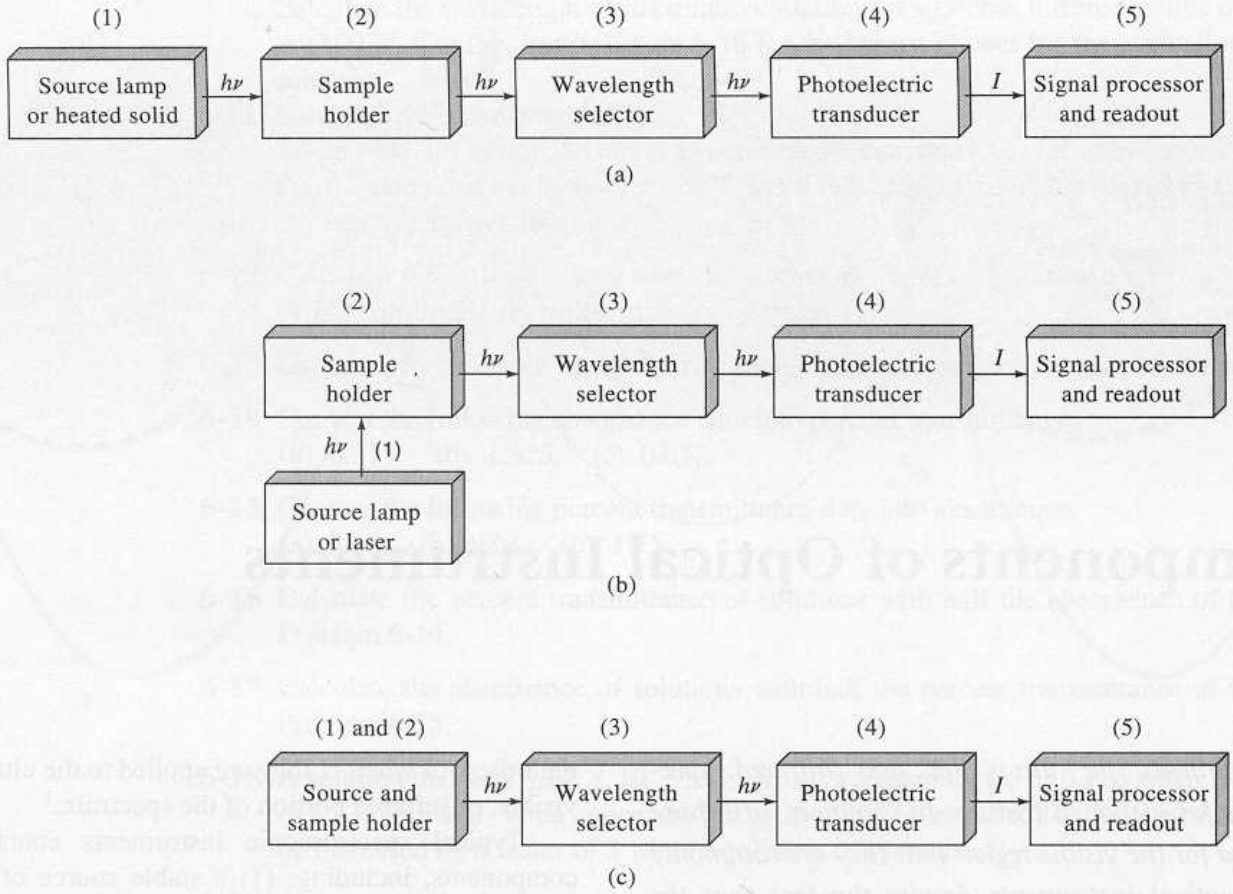

Figure 7-1 Components of various types of instruments for optical spectroscopy: (a) absorption; (b) fluorescence, phosphorescence, and scattering; (c) emission and chemiluminescence.

The first two instrumental configurations, which are used for the measurement of absorption, fluorescence, phosphorescence, and scattering, require an external source of radiant energy. For absorption, the beam from the source passes through the sample directly into the wavelength selector, although in some instruments, the position of the sample and selector is reversed. In the latter three, the source induces the sample, held in a container, to emit characteristic fluorescence, phosphorescence, or scattered radiation, which is usually measured at an angle of 90 deg with respect to the source.

Emission spectroscopy and chemiluminescence spectroscopy differ from the other types in the respect that no external radiation source is required; the sample itself is the emitter (see Figure 7-1c). In emission spectroscopy, the sample container is an arc, a spark, or a flame that both holds the sample and causes it to emit characteristic radiation. In chemiluminescence spectroscopy, the radiation source is a solution of the analyte plus reagents held in a glass sample holder. Emission is brought about by energy released in a chemical reaction in which the analyte takes part directly or indirectly.

Figures 7-2 and 7-3 summarize the optical characteristics of all the components shown in Figure 7-1 with the exception of the signal processor and readout. Note that instrument components differ in detail, depending upon the wavelength region within which they are to be used. Their design also depends on whether the instrument is to be used primarily for qualitative or quantitative analysis and on whether it is to be applied to atomic or molecular spectroscopy. Nevertheless, the general function and performance requirements of each type of component are similar, regardless of wavelength region and application.

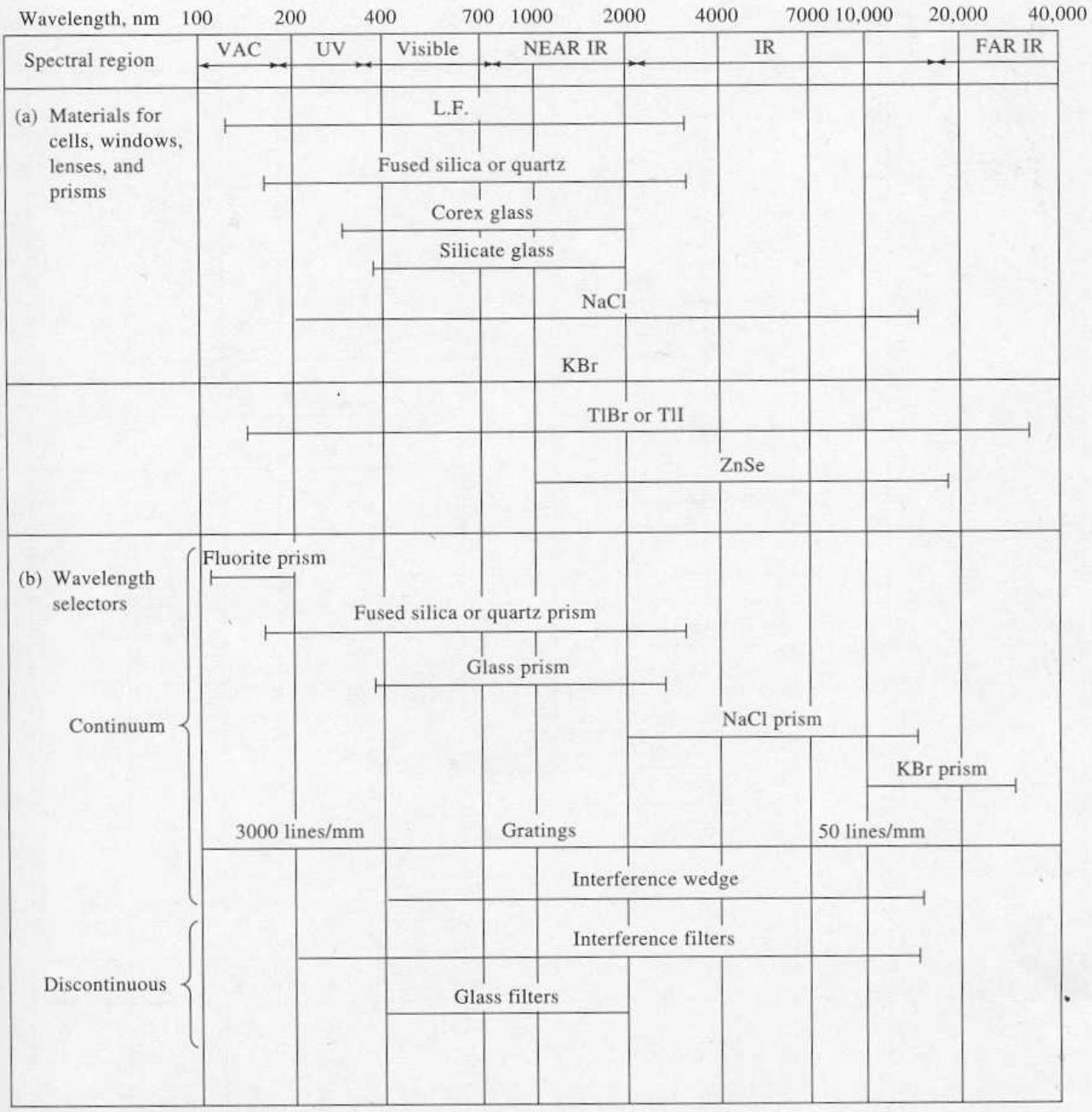

Figure 7-2 (a) Construction materials and (b) wavelength selectors for spectroscopic instruments.

7B SOURCES OF RADIATION

In order to be suitable for spectroscopic studies, a source must generate a beam of radiation with sufficient power for easy detection and measurement. In addition, its output power should be stable for reasonable periods. Typically, the radiant power of a source varies exponentially with the voltage of its power supply. Thus, a regulated power source is often needed to provide the required stability. Alternatively, the problem of source stability is circumvented by double-beam designs in which the ratio of the signal from the sample to that of the source in the absence of sample serves as the analytical variable. In such designs, the intensities of the two beams are measured si-

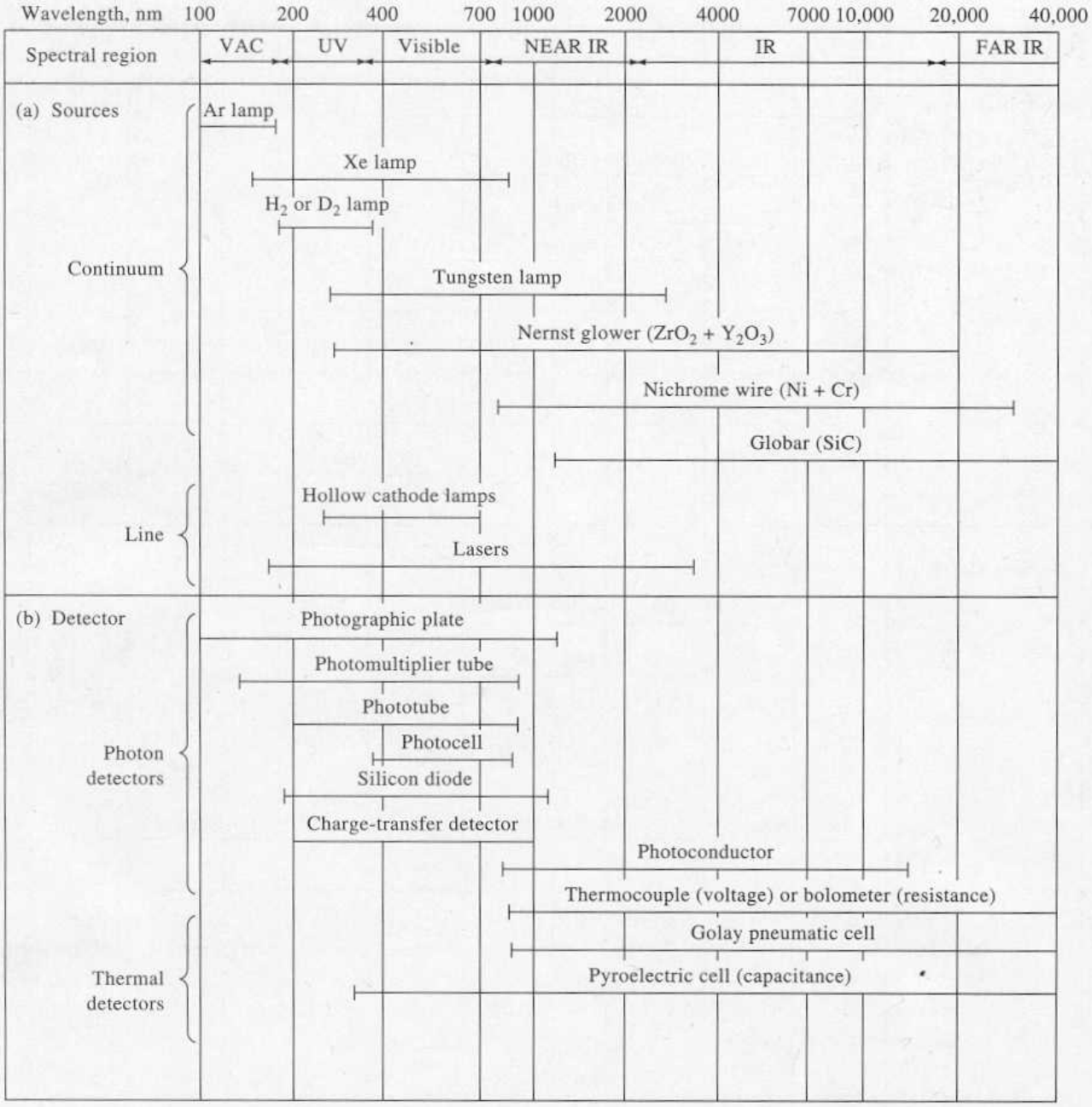

Figure 7-3 (a) Sources and (b) detectors for spectroscopic instruments.

multaneously or nearly simultaneously so that the effect of fluctuations in the source output is largely canceled.

Figure 7-3a lists the most widely used spectroscopic sources. Note that these sources are of two types: *continuum sources,* which emit radiation that changes in intensity only slowly as a function of wavelength, and *line sources,* which emit a limited number of lines or bands of radiation each of which spans a limited range of wavelengths.

7B-1 Continuum Sources

Continuum sources find widespread use in absorption and fluorescence spectroscopy. For the ultraviolet region, the most common source is the deuterium lamp. High-pressure, gas-filled arc lamps that contain argon, xenon, or mercury serve when a particularly intense source is required. For the visible region of the spectrum, the tungsten filament lamp is used almost univer-

sally. The common infrared sources are inert solids heated to 1500 to 2000 K, a temperature at which the maximum radiant output occurs at 1.5 to 1.9 μm (see Figure 6-18). Details on the construction and behavior of these various continuum sources will be found in the chapter dealing with specific types of spectroscopic methods.

7B-2 Line Sources

Sources that emit a few discrete lines find wide use in atomic absorption spectroscopy, atomic and molecular fluorescence spectroscopy, and Raman spectroscopy (refractometry and polarimetry also employ line sources). The familiar mercury and sodium vapor lamps provide a relatively few sharp lines in the ultraviolet and visible regions and are used in several spectroscopic instruments. Hollow cathode lamps and electrodeless discharge lamps are the most important line sources for atomic absorption and fluorescence methods. Discussion of such sources is deferred to Section 9B-1.

7B-3 Laser Sources

Lasers are highly useful sources in analytical instrumentation because of their high intensities, their narrow bandwidths, and the coherent nature of their outputs.[3] The first laser was described in 1960. Since that time, chemists have found numerous useful applications for these sources in high-resolution spectroscopy, in kinetic studies of processes with lifetimes in the range of 10^{-9} to 10^{-12} s, in the detection and determination of extremely small concentrations of species in the atmosphere, and in the induction of isotopically selective reactions.[4] In addition, laser sources have become important in several routine analytical methods, including Raman spectroscopy, molecular absorption spectroscopy, emission spectroscopy, and as part of instruments for Fourier transform infrared spectroscopy.

The term *laser* is an acronym for **l**ight **a**mplification by **s**timulated **e**mission of **r**adiation. As a consequence of their light-amplifying characteristics, lasers produce spatially narrow (a few hundredths of a micrometer), extremely intense beams of radiation. The process of stimulated emission, which will be described shortly, produces a beam of highly monochromatic (bandwidths of 0.01 nm or less) and remarkably coherent (Section 6B-6) radiation. Because of these unique properties, lasers have become important sources for use in the ultraviolet, visible, and infrared regions of the spectrum. A limitation of early lasers was that the radiation from a given source was restricted to a relatively few discrete wavelengths or lines. Now, however, dye lasers are available that provide narrow bands of radiation at any chosen wavelength within a somewhat limited range of the source.

Components of Lasers

Figure 7-4 is a schematic representation that shows the components of a typical laser source. The heart of the device is the lasing medium. It may be a solid crystal such as ruby, a semiconductor such as gallium arsenide, a solution of an organic dye, or a gas such as argon or krypton. The lasing material is often activated, or *pumped,* by radiation from an external source so that a few photons of proper energy will trigger the formation of a cascade of photons of the same energy. Pumping can also be accomplished by an electrical current or by an electrical discharge. Thus, gas lasers usually do not have the external radiation source shown in Figure 7-4; instead, the power supply is connected to a pair of electrodes contained in a cell filled with the gas.

A laser normally functions as an oscillator, or a resonator, in the sense that the radiation produced by the lasing action is caused to pass back and forth through the medium numerous times by means of a pair of mirrors as shown in Figure 7-4. Additional photons are generated with each passage, thus leading to enormous amplification. The repeated passage also produces a beam that is highly parallel because nonparallel radiation escapes from the sides of the medium after being reflected a few times (see Figure 7-4). One of the easiest ways to obtain a usable laser beam is to coat one of the mirrors with a sufficiently thin layer of reflecting mate-

---

[3] For a more complete discussion of lasers, see J. Wilson and J. F. B. Hawkes, *Lasers: Principles and Applications.* Englewood Cliffs, NJ: Prentice-Hall, 1987; D. L. Andrews, *Lasers in Chemistry.* New York: Springer-Verlag, 1986; *Laser Spectroscopy and Its Applications,* L. Radziemski, R. Solarz, and J. Paisner, Eds. New York: Marcel Dekker, 1987; *Applications of Lasers,* E. Piepmeier, Ed. New York: Wiley, 1986.

[4] For reviews of some of these applications, see J. C. Wright and M. J. Wirth, *Anal. Chem.,* **1980**, *52,* 988A, 1087A; A. Schawlow, *Science,* **1982**, *217,* 9; E. W. Findsend and M. R. Ondrias, *J. Chem. Educ.,* **1986**, *63,* 479; R. N. Zare, *Science,* **1984**, *226,* 1198; C. P. Christensen, *Science,* **1984**, *224,* 117; J. K. Steehler, *J. Chem. Educ.,* **1990**, *67,* A37.

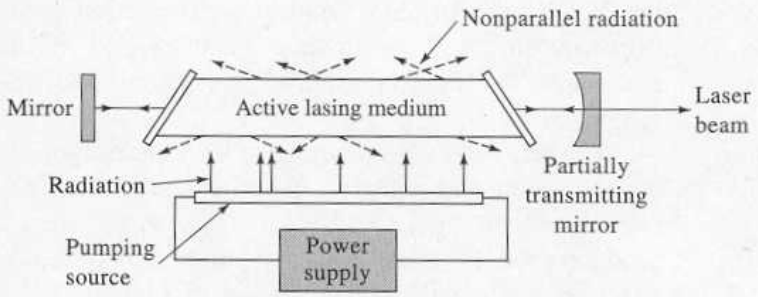

Figure 7-4 Schematic representation of a typical laser source.

rial so that a fraction of the beam is transmitted rather than reflected.

Mechanism of Laser Action

Laser action can be understood by considering the four processes depicted in Figure 7-5, namely: (a) pumping, (b) spontaneous emission (fluorescence), (c) stimulated emission, and (d) absorption. In this figure, we show the behavior of two of the many molecules that make up the lasing medium. Two of the several electronic energy levels of each are shown as having energies E_y and E_x. Note that the higher electronic state for each molecule has several slightly different vibrational energy levels depicted as E_y, E_y', E_y'', and so forth. We have not shown additional levels for the lower electronic state, although such usually exist.

Pumping. Pumping, which is necessary for laser action, is a process by which the active species of a laser is excited by means of an electrical discharge, passage of an electrical current, or exposure to an intense radiant source. During pumping, several of the higher electronic and vibrational energy levels of the active species are populated. In diagram (1) of Figure 7-5a, one molecule is shown as being promoted to an energy state E_y''; the second is excited to the slightly higher vibrational level E_y'''. The lifetime of excited *vibrational* states is brief, and after 10^{-13} to 10^{-15} s, relaxation to the lowest excited vibrational level [E_y in diagram a(3)] occurs with the production of an undetectable quantity of heat. Some excited electronic states of laser materials have lifetimes considerably longer (often 1 ms or more) than their excited vibrational counterparts; long-lived states are sometimes termed *metastable* as a consequence.

Spontaneous Emission. As was pointed out in the discussion of fluorescence (page 137), a species in an excited electronic state may lose all or part of its excess energy by spontaneous emission of radiation. This process is depicted in the three diagrams shown in Figure 7-5b. Note that the wavelength of the fluorescence radiation is given by the relationship $\lambda = hc/(E_y - E_x)$ where h is the Planck constant and c is the speed of light. It is also important to note that the instant at which emission occurs and the path of the resulting photon vary from excited molecule to excited molecule because spontaneous emission is a random process; thus, as shown in Figure 7-5, the fluorescence radiation produced by one of the species in diagram b(1) differs in direction and phase from that produced by the second species [diagram b(2)]. Spontaneous emission, therefore, yields *incoherent* monochromatic radiation.

Stimulated Emission. Stimulated emission, which is the basis of laser behavior, is depicted in Figure 7-5c. Here, the excited laser species are struck by photons that have precisely the same energies $(E_y - E_x)$ as the photons produced by spontaneous emission. Collisions of this type cause the excited species to relax immediately to the lower energy state and to simultaneously emit a photon of exactly the same energy as the photon that stimulated the process. Equally important, the emitted photon *travels* in exactly the same direction and *is precisely in phase* with the photon that caused the emission. Therefore, the stimulated emission is totally *coherent* with the incoming radiation.

Absorption. The absorption process, which competes with stimulated emission, is depicted in Figure 7-5d. Here, two photons with energies exactly equal to $(E_y - E_x)$ are absorbed to produce the metastable excited state shown in diagram d(3); note that the state shown in diagram d(3) is identical to that attained in diagram a(3) by pumping.

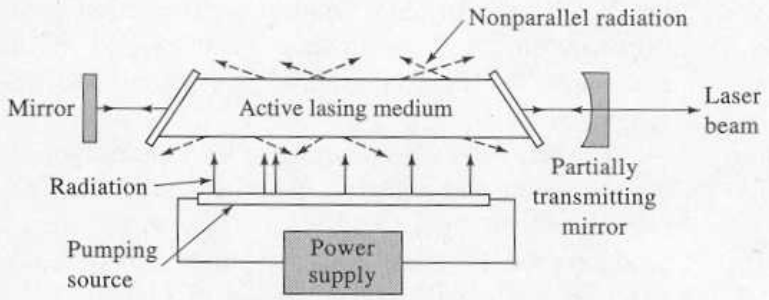

Figure 7-4 Schematic representation of a typical laser source.

rial so that a fraction of the beam is transmitted rather than reflected.

Mechanism of Laser Action

Laser action can be understood by considering the four processes depicted in Figure 7-5, namely: (a) pumping, (b) spontaneous emission (fluorescence), (c) stimulated emission, and (d) absorption. In this figure, we show the behavior of two of the many molecules that make up the lasing medium. Two of the several electronic energy levels of each are shown as having energies E_y and E_x. Note that the higher electronic state for each molecule has several slightly different vibrational energy levels depicted as E_y, E_y', E_y'', and so forth. We have not shown additional levels for the lower electronic state, although such usually exist.

Pumping. Pumping, which is necessary for laser action, is a process by which the active species of a laser is excited by means of an electrical discharge, passage of an electrical current, or exposure to an intense radiant source. During pumping, several of the higher electronic and vibrational energy levels of the active species are populated. In diagram (1) of Figure 7-5a, one molecule is shown as being promoted to an energy state E_y''; the second is excited to the slightly higher vibrational level E_y'''. The lifetime of excited *vibrational* states is brief, and after 10^{-13} to 10^{-15} s, relaxation to the lowest excited vibrational level [E_y in diagram a(3)] occurs with the production of an undetectable quantity of heat. Some excited electronic states of laser materials have lifetimes considerably longer (often 1 ms or more) than their excited vibrational counterparts; long-lived states are sometimes termed *metastable* as a consequence.

Spontaneous Emission. As was pointed out in the discussion of fluorescence (page 137), a species in an excited electronic state may lose all or part of its excess energy by spontaneous emission of radiation. This process is depicted in the three diagrams shown in Figure 7-5b. Note that the wavelength of the fluorescence radiation is given by the relationship $\lambda = hc/(E_y - E_x)$ where h is the Planck constant and c is the speed of light. It is also important to note that the instant at which emission occurs and the path of the resulting photon vary from excited molecule to excited molecule because spontaneous emission is a random process; thus, as shown in Figure 7-5, the fluorescence radiation produced by one of the species in diagram b(1) differs in direction and phase from that produced by the second species [diagram b(2)]. Spontaneous emission, therefore, yields *incoherent* monochromatic radiation.

Stimulated Emission. Stimulated emission, which is the basis of laser behavior, is depicted in Figure 7-5c. Here, the excited laser species are struck by photons that have precisely the same energies $(E_y - E_x)$ as the photons produced by spontaneous emission. Collisions of this type cause the excited species to relax immediately to the lower energy state and to simultaneously emit a photon of exactly the same energy as the photon that stimulated the process. Equally important, the emitted photon *travels* in exactly the same direction and *is precisely in phase* with the photon that caused the emission. Therefore, the stimulated emission is totally *coherent* with the incoming radiation.

Absorption. The absorption process, which competes with stimulated emission, is depicted in Figure 7-5d. Here, two photons with energies exactly equal to $(E_y - E_x)$ are absorbed to produce the metastable excited state shown in diagram d(3); note that the state shown in diagram d(3) is identical to that attained in diagram a(3) by pumping.

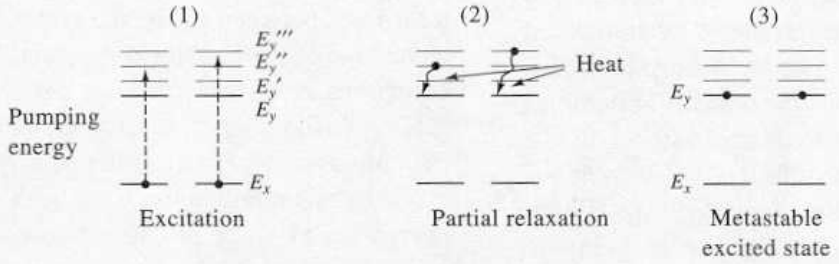

(a) Pumping (excitation by electrical, radiant, or chemical energy)

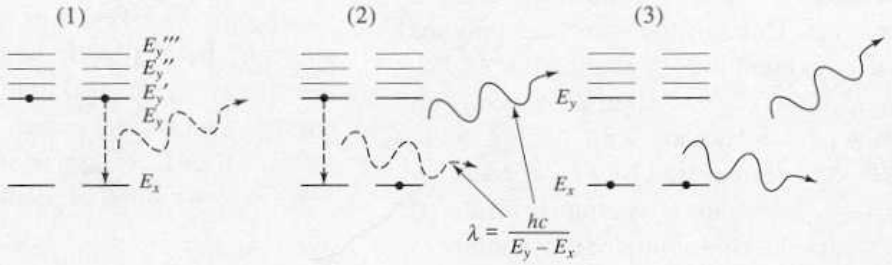

(b) Spontaneous emission

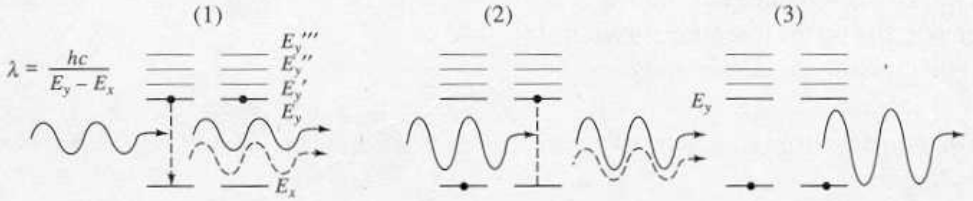

(c) Stimulated emission

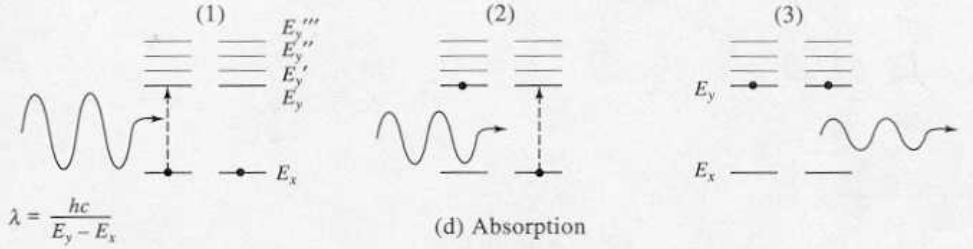

(d) Absorption

Figure 7-5 Four processes important in laser action: (a) pumping (excitation by electrical, radiant, or chemical energy), (b) spontaneous emission, (c) stimulated emission, and (d) absorption.

Population Inversion and Light Amplification

In order to have light amplification in a laser, it is necessary that the number of photons produced by stimulated emission exceed the number lost by absorption. This condition will prevail only when the number of particles in the higher energy state exceeds the number in the lower; in other words, there must be a *population inversion* from the normal distribution of energy states. Population inversions are brought about by pumping. Figure 7-6 contrasts the effect of incoming radiation on a noninverted population with that of an inverted one. In each case the population is shown as being made up of nine molecules of the lasing medium. In the noninverted system, three molecules are in the excited state and six are in the lower energy level. Three of the incoming photons are absorbed by the medium, thus producing three additional excited molecules. The radiation also, however, stimulates emission of two photons from excited molecules. Thus, the beam is attenuated by one photon. As shown in Figure 7-5b, a net gain in photons is observed in the inverted system because stimulated emission goes on to a greater extent than absorption does.

Three- and Four-Level Laser Systems

Figure 7-7 shows simplified energy diagrams for the two common types of laser systems. In the three-level system, the transition responsible for laser radiation is between an excited state E_y and the ground state E_0; in a four-level system, on the other hand, radiation is generated by a transition from E_y to a state E_x that has a greater energy than the ground state. Furthermore, it is necessary that transitions between E_x and the ground state be rapid. The advantage of the four-level system is that the population inversions necessary for laser action are more readily achieved. To understand this fact, note that at room temperature a large majority of the laser species will be in the ground-state energy level E_0 in both systems. Sufficient energy must thus be provided to convert more than 50% of the lasing species to the E_y level of a three-level system. In contrast, it is only necessary to pump sufficiently to make the number of particles in the E_y energy level exceed the number in E_x of a four-level system. The lifetime of a particle in the E_x state is brief, however, because the transition to E_0 is fast; thus, the number in the E_x state will generally be negligible with respect to the number that has energy E_0 and also (with a modest input of pumping energy) with respect to the number in the E_y state. Therefore, the four-level laser usually achieves a population inversion with a small expenditure of pumping energy.

Some Examples of Useful Lasers[5]

Solid State Lasers. The first successful laser, and one that still finds widespread use, is a three-level device in which a ruby crystal is the active medium. Ruby is pri-

[5] For a review of lasers that are useful in analytical chemistry, see J. C. Wright and M. J. Wirth, *Anal. Chem.*, **1980**, *52*, 1087A.

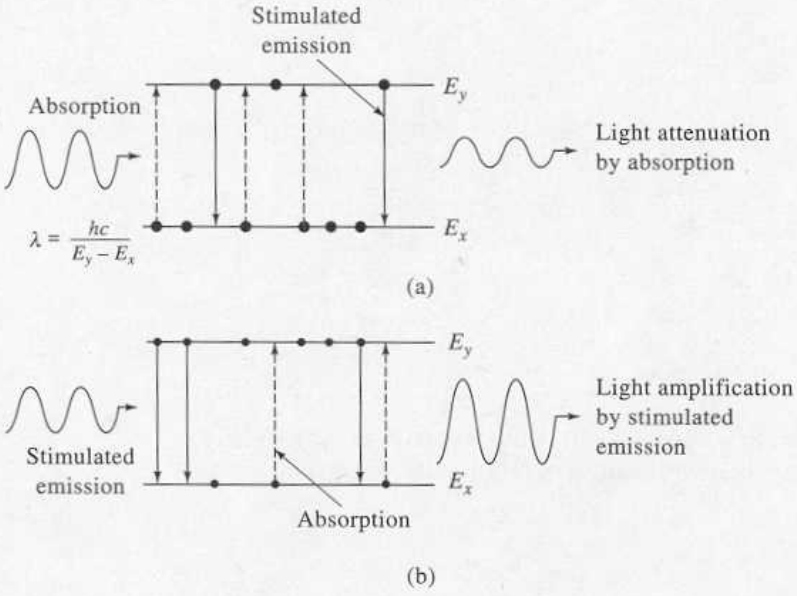

Figure 7-6 Passage of radiation through (a) a noninverted population and (b) an inverted population.

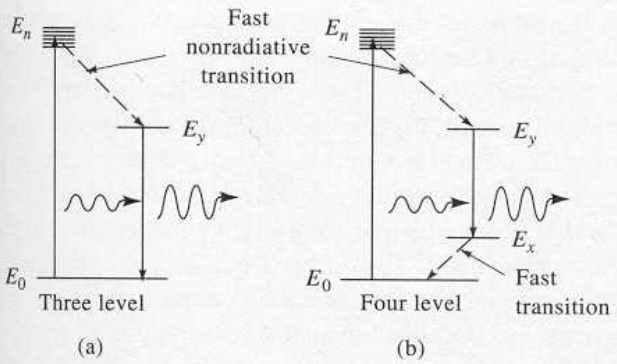

Figure 7-7 Energy level diagrams for two types of laser systems.

marily Al_2O_3 but contains approximately 0.05% chromium(III) distributed among the aluminum(III) lattice sites, which accounts for the red coloration. The chromium(III) ions are the active lasing material. In early lasers, the ruby was machined into a rod about 4 cm in length and 0.5 cm in diameter. A flash tube (often a low-pressure xenon lamp) was coiled around the cylinder to produce intense flashes of light (λ = 694.3 nm). Because the pumping was discontinuous, a pulsed beam was produced. Continuous-wave ruby sources are now available.

The Nd:YAG laser is one of the most widely used solid-state lasers. It consists of neodymium ion in a host crystal of yttrium aluminum garnet. This system offers the advantage of being a four-level laser, which makes it much easier to achieve population inversion than with the ruby laser. The Nd:YAG laser has a very high radiant power output at 1064 nm, which is usually frequency doubled (see page 154) to give an intense line at 532 nm. This radiation is often used for pumping tunable dye lasers.

Gas Lasers. A variety of gas lasers are available commercially. These devices are of four types: (1) neutral atom lasers such as He/Ne; (2) ion lasers in which the active species is Ar^+ or Kr^+; (3) molecular lasers in which the lasing medium is CO_2 or N_2; and (4) eximer lasers. The helium/neon laser is the most widely encountered of all lasers because of its low initial and maintenance costs, its great reliability, and its low power consumption.[6] The most important of its output lines is at 632.8 nm. It is generally operated in the continuous mode rather than a pulsed mode.

The argon ion laser, which produces intense lines in the green (514.5 nm) and the blue (488.0 nm) regions, is an important example of an ion laser. This laser is a four-level device in which argon ions are formed by an electrical or radio-frequency discharge. The required input energy is high because the argon atoms must first be ionized and then excited from their ground state, with a principal quantum number of 3, to various 4*p* states. Laser activity occurs when the excited ions relax to the 4*s* state. The argon ion laser finds use as a source in fluorescence and Raman spectroscopy because of the high intensity of its lines.

The N_2 laser, which must be operated in the pulsed mode because pumping is carried out with a high potential spark source, provides intense radiation at 337.1 nm. This output has found extensive use for exciting fluorescence in a variety of molecules and for pumping dye lasers. The CO_2 gas laser is used to produce monochromatic infrared radiation at 10.6 μm.

Eximer lasers contain a gaseous mixture of helium, fluorine, and one of the rare gases argon, krypton, or xenon. The rare gas is electronically excited by an electrical current whereupon it reacts with the fluorine to form excited ions such as ArF^+, KrF^+, or XeF^+, which are called *eximers* because they are stable only in the excited state. Since the eximer ground state is unstable, rapid dissociation of the compounds occurs as they relax while giving off a photon. Thus, there is a population inversion as long as pumping is carried on. Eximer lasers produce high energy pulses in ultraviolet (351 nm for XeF, 248 nm for KrF, and 193 nm for ArF).

Dye Lasers.[7] Dye lasers have become important radiation sources in analytical chemistry because they are continuously tunable over a range of 20 to 50 nm. The bandwidth of a tunable laser is typically a few hundredths of a nanometer or less. The active materials in dye lasers are solutions of organic compounds capable of fluorescing in the ultraviolet, visible, or infrared regions. Dye lasers are four-level systems. In contrast to the other lasers of this type that we have considered, however, the lower energy level for laser action (E_x in Figure 7-6b) is

[6] For details on the design of commercial He/Ne lasers, see B. Patel, *Photonics Spectra*, **1983** (1), 33.

[7] For further information, see R. B. Green, *J. Chem. Educ.*, **1977**, *54*, A365, A407; M. J. Wirth, *Tunable Laser Systems* in *Lasers in Chemical Analysis*, G. M. Hieftje, J. C. Travis, and F. E. Lytle, Eds. Clifton, NJ: Humana Press, 1981.

not a single energy but a band of energies that arise from the superposition of a large number of closely spaced vibrational and rotational energy states upon the base electronic energy state. Electrons in E_y may then undergo transitions to any of these states, thus producing photons of slightly different energies. Tuning of dye lasers can be readily accomplished by replacing the nontransmitting mirror shown in Figure 7-4 with a monochromator equipped with a reflection grating or a Littrow-type prism (see Figure 7-16) that reflects only a narrow bandwidth of radiation into the laser medium; the peak wavelength can be varied by rotation of the grating or prism. Emission is then stimulated for only part of the fluorescence spectrum, namely, the wavelength selected by the monochromator.

Semiconductor Diode Lasers.[8] A new and increasingly important source of nearly monochromatic radiation is the laser diode. Laser diodes are products of modern semiconductor technology. Their mechanism of operation may be understood by considering the electrical conduction characteristics of various materials as illustrated in Figure 7-8. A good conductor, such as a metal, consists of a regular arrangement of atoms immersed in a sea of valence electrons. Orbitals on adjacent atoms overlap to form the so-called *valence band,* which is essentially a molecular orbital over the entire metal and which contains the valence electrons of all of the atoms. Empty outer orbitals overlap to form the *conduction band,* which lies at a slightly higher energy than the valence band. The difference in energy between the valence band and the conduction band is the band-gap energy, E_g. Because the band-gap energy is so small in conductors (see Figure 7-8a), electrons in the valence band easily acquire sufficient thermal energy to be promoted to the conduction band, thus providing mobile charge carriers for conduction.

In contrast, insulators have a relatively large band-gap energy, and as a result, electrons in the valence band are unable to acquire enough thermal energy to make the transition to the conduction band, and thus insulators do not conduct electricity (see Figure 7-8c). Semiconductors, such as silicon or germanium, have intermediate band-gap energies, and thus their conduction characteristics are intermediate between conductors and insulators (see Figure 7-8b). We should note that whether a material is a semiconductor or an insulator depends not only on the band-gap energy but also on the temperature of operation and the energy of excitation of the material, which is related to the voltage applied to the material.

When a voltage is impressed across a semiconductor diode in the forward direction (see Section 2C-2),

[8] M. G. D. Bauman, J. C. Wright, A. B. Ellis, T. Kuech, and G. C. Lisensky, *J. Chem. Educ.*, 1992, *69*, 89; T. Imasaka and N. Ishibashi, *Anal. Chem.*, 1990, *62*, 363A; R. L. Beyer, *Science*, 1989, *239*, 742; K. Niemax, A. Zybin, C. Schnürer-Patschan, and H. Groll, *Anal. Chem.*, 1996, *68*, 351A.

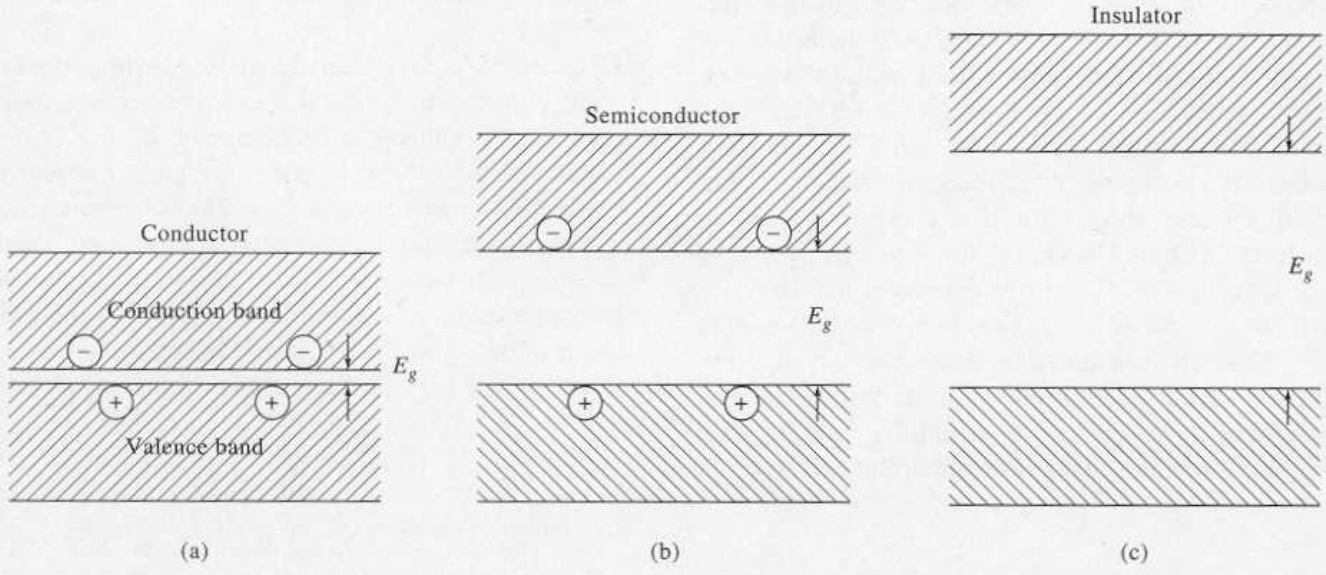

Figure 7-8 Conduction bands and valence bands in three types of materials.

electrons are excited into the conduction band, hole-electron pairs are created, and the diode conducts. Ultimately, some of these electrons relax and go back into the valence band, and energy is released that corresponds to the band-gap energy $E_g = h\nu$. Some of the energy is released in the form of electromagnetic radiation of frequency $\nu = E_g/h$. Diodes that are fabricated to enhance the production of light are called *light-emitting diodes,* or LEDs. Light-emitting diodes are often made of gallium arsenide that is doped with phosphorus, which has a band-gap energy that corresponds to a wavelength of 660 nm. Diodes of this type find wide use as indicators and readouts in electronic instruments. Unfortunately, because of their relatively low intensity and emission wavelengths in the red and infrared, LEDs are of limited utility in spectroscopy.

In recent years semiconductor fabrication techniques have progressed to an extent that permits the construction of highly complex integrated devices such as the distributed-Bragg-reflector (DBR) laser diode shown in Figure 7-9. This device contains a gallium arsenide *pn*-junction diode that produces infrared radiation at about 975 nm. In addition, a stripe of material is fabricated on the chip that acts as a resonant cavity for the radiation so that light amplification can occur within the cavity. An integrated grating provides feedback to the resonant cavity so that the resulting radiation has an extremely narrow bandwidth of about 10^{-5} nm. Laser diodes of this type have achieved continuous power outputs of more than 100 mW with a typical thermal stability of 0.1 nm/°C. Laser diodes may be operated in either a pulsed or continuous (CW) mode, which increases their versatility in a variety of applications. Rapid development of laser diodes has resulted from their utility as light sources for compact-disk players, CD-ROM drives, bar-code scanners, and other familiar optoelectronic devices, and mass production of laser diodes ensures that their cost will continue to be low.

A major impediment to the use of laser diodes in spectroscopic applications has been their limited wavelength range in the red and infrared regions of the spectrum. This disadvantage may be overcome by operating the laser diode in the pulsed mode to achieve sufficient peak power to use nonlinear optics to provide frequency doubling as shown in Figure 7-10. Here, the output of a laser diode is focused in a doubling crystal to provide output in the blue-green region of the spectrum (~490 nm). With proper external optics, frequency-doubled laser diodes can achieve average output powers of 0.5 to 1.0 W with a tunable spectral range of about 30 nm. The advantages of such light sources include compactness, power efficiency, high reliability, and ruggedness. The addition of external optics to the laser diode increases the cost of the devices substantially, but they are competitive with larger, less efficient, and less reliable gas-based lasers.

Recently, it has been reported that gallium nitride laser diodes produce radiation directly in the blue, green, and yellow region of the spectrum.[9] These diodes should prove useful for spectroscopic studies.

The utility of laser diodes for spectroscopic applications has been demonstrated in molecular absorption spectrometry, molecular fluorescence spectrometry, atomic absorption spectrometry, and as light sources for detectors in various chromatographic methods. As practical diode lasers achieve wide commercial availability, they will doubtless appear in increasing numbers as light sources in commercial spectrometric systems.

[9] G. Fasol, *Science,* **1996**, *272,* 1751.

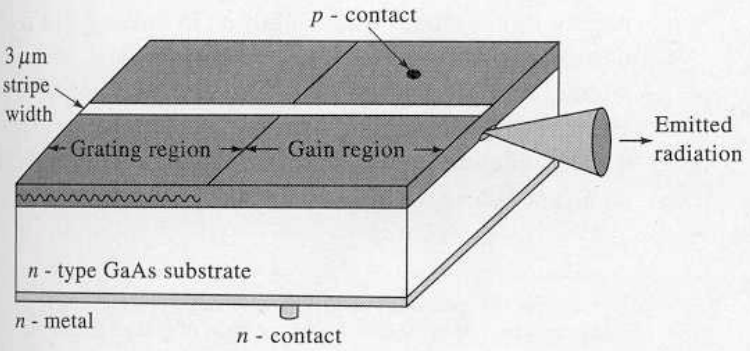

Figure 7-9 A distributed Bragg-reflector laser diode. *(From D. W. Nam and R. G. Waarts,* Laser Focus World, ***1994,*** *30(8), 52. With permission.)*

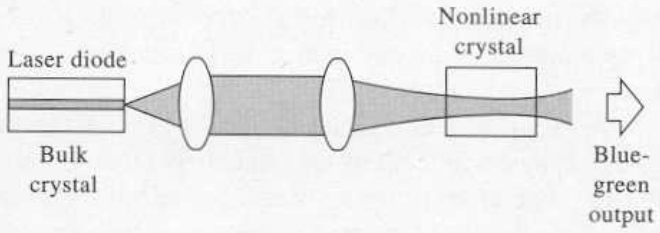

Figure 7-10 A frequency-doubled system for converting 975-nm laser output to 490 nm. *(From D. W. Nam and R. G. Waarts,* Laser Focus World, ***1994,*** *30(8), 52. With permission.)*

Nonlinear Optical Effects with Lasers

As we have noted in Section 6B-7, when an electromagnetic wave is transmitted through a dielectric[10] medium, the electromagnetic field of the radiation causes momentary distortion, or polarization, of the valence electrons of the molecules that make up the medium. For ordinary radiation the extent of polarization P is directly proportional to the magnitude of the electrical field E of the radiation. Thus we may write

$$P = \alpha E$$

where α is the proportionality constant. Optical phenomena that occur when this situation prevails are said to be *linear.*

At the high radiation intensities encountered with lasers, this relationship breaks down, particularly when E approaches the binding energy of the electrons. Under these circumstances, *nonlinear optical effects* are observed wherein the relationship between polarization and electrical field is given by the equation

$$P = \alpha E + \beta E^2 + \gamma E^3 + \ldots \qquad (7\text{-}1)$$

where the magnitude of the three constants are in the order $\alpha > \beta > \gamma$. At ordinary radiation intensities, only the first term on the right is significant, and the relationship between polarization and field strength is linear. With high-intensity lasers, however, the second term and sometimes even the third term are required to describe the degree of polarization. When only two terms are required, Equation 7-1 can be rewritten in terms of radiation frequency ω and the maximum amplitude of the field strength, E_m. Thus,

$$P = \alpha E_m \sin \omega t + \beta E_m^2 \sin^2 \omega t \qquad (7\text{-}2)$$

Substituting the trigonometric identity $\sin^2 \omega t = \frac{1}{2}(1 - \cos 2\omega t)$ gives

$$P = \alpha E_m \sin \omega t + \frac{\beta E_m^2}{2}(1 - \cos 2\omega t) \qquad (7\text{-}3)$$

The first term in Equation 7-3 is the normal linear term that predominates at low radiation intensities. At sufficiently high intensity, the second-order term becomes significant and results in radiation that has a frequency 2ω that is *double* that of the incident radiation. This frequency-doubling process is now widely used to produce laser frequencies of shorter wavelengths. For example, the 1064-nm near-infrared radiation from a Nd:YAG laser can be frequency doubled to produce a 30% yield of green radiation at 532 nm by passing the radiation through a crystalline material such as potassium dihydrogen phosphate. The 532-nm radiation can then be doubled again to yield ultraviolet radiation at 266 nm by passage through a crystal of ammonium dihydrogen phosphate.

Radiation from laser sources is beginning to find application in several types of nonlinear spectroscopy, most notably in Raman spectroscopy (see Section 18D-3).

7C WAVELENGTH SELECTORS

For most spectroscopic analyses, radiation that consists of a limited, narrow, continuous group of wavelengths called a *band* is required.[11] A narrow bandwidth enhances the sensitivity of absorbance measurements, may provide selectivity to both emission and absorption methods, and is frequently a requirement from the standpoint of obtaining a linear relationship between the optical signal and concentration (Equation 6-34). Ideally, the output from a wavelength selector would be radiation of a single wavelength or frequency. No real wavelength selector even approaches this ideal; instead, a band, such as that shown in Figure 7-11, is obtained. Here, the percentage of incident radiation of a given wavelength that is transmitted by the selector is plotted as a function of wavelength. The *effective bandwidth,*

[10] Dielectrics are a class of substances that are nonconductors because they contain no free electrons. Generally, dielectrics are optically transparent in contrast to electrically conducting solids, which either absorb radiation or reflect it strongly.

[11] Note that the term *band* in this context has a somewhat different meaning from that used in describing types of spectra in Chapter 6.

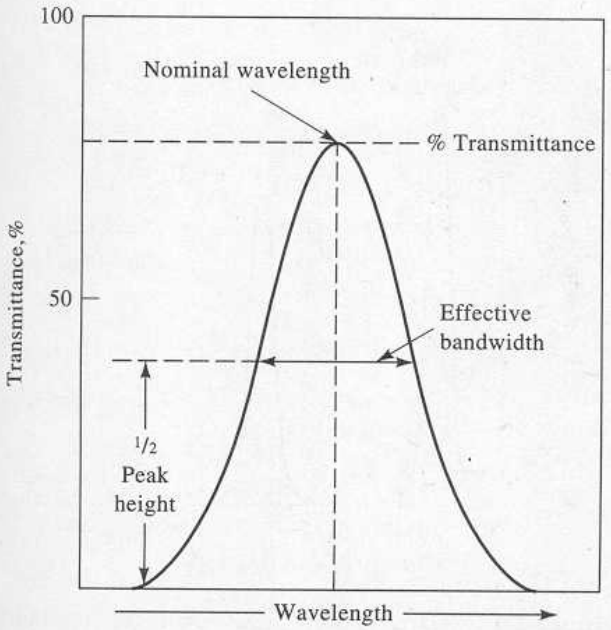

Figure 7-11 Output of a typical wavelength selector.

which is defined in Figure 7-11, is an inverse measure of the quality of the device, a narrower bandwidth representing better performance. Two types of wavelength selectors are encountered, filters and monochromators.

7C-1 Filters

Two types of filters are employed for wavelength selection: *interference filters* and *absorption filters* (the former are sometimes called *Fabry-Perot filters*). Absorption filters are restricted to the visible region of the spectrum; interference filters, on the other hand, are available for the ultraviolet, visible, and well into the infrared region.

Interference Filters

As the name implies, interference filters rely on optical interference to provide narrow bands of radiation. An interference filter consists of a transparent dielectric[12] (frequently calcium fluoride or magnesium fluoride) that occupies the space between two semitransparent metallic films. This array is sandwiched between two plates of glass or other transparent materials (see Figure 7-12a). The thickness of the dielectric layer is carefully controlled and determines the wavelength of the transmitted radiation. When a perpendicular beam of collimated radiation strikes this array, a fraction passes through the first metallic layer while the remainder is reflected. The portion that is passed undergoes a similar partition when it strikes the second metallic film. If the reflected portion from this second interaction is of the proper wavelength, it is partially reflected from the inner side of the first layer in phase with incoming light of the same wavelength. The result is that this particular wavelength is reinforced, while most other wavelengths, being out of phase, suffer destructive interference.

The relationship between the thickness of the dielectric layer t and the transmitted wavelength λ can be found with the aid of Figure 7-12b. For purposes of clarity, the incident beam is shown as arriving at an angle θ from the perpendicular. At point 1, the radiation is partially reflected and partially transmitted to point 1′ where partial reflection and transmission again takes

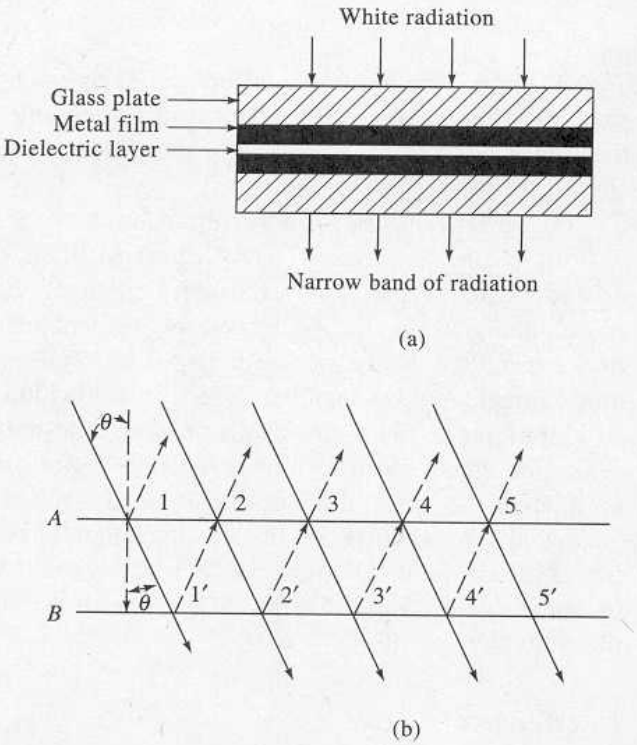

Figure 7-12 (a) Schematic cross section of an interference filter. Note that the drawing is not to scale and that the three central bands are much narrower than shown. (b) Schematic to show the conditions for constructive interference.

[12] A dielectric material is an insulator that contains essentially no current-carrying charged particles. Dielectors are generally transparent in most spectral regions.

place. The same process occurs at 2, 2′, and so forth. For reinforcement to occur at point 2, the distance traveled by the beam reflected at 1′ must be some multiple of its wavelength in the medium λ′. Since the path length between surfaces can be expressed as $t/\cos\theta$, the condition for reinforcement is that

$$\mathbf{n}\lambda' = 2t/\cos\theta$$

where **n** is a small whole number.

In ordinary use, θ approaches zero and cos θ approaches unity so that the foregoing equation simplifies to

$$\mathbf{n}\lambda' \approx 2t \qquad (7\text{-}4)$$

where λ′ is the wavelength of radiation *in the dielectric* and t is the thickness of the dielectric. The corresponding wavelength in air is given by

$$\lambda = \lambda'\eta$$

where η is the refractive index of the dielectric medium. Thus, the wavelengths of radiation transmitted by the filter are

$$\lambda = \frac{2t\eta}{\mathbf{n}} \qquad (7\text{-}5)$$

The integer **n** is the *order* of interference. The glass layers of the filter are often selected to absorb all but one of the reinforced bands; transmission is thus restricted to a single order.

Figure 7-13 illustrates the performance characteristics of typical interference filters. Ordinarily, filters are characterized, as shown, by the wavelength of their transmittance peaks, the percentage of incident radiation transmitted at the peak (their *percent transmittance,* Equation 6-31), and their effective bandwidths.

Interference filters are available with transmitter peaks throughout the ultraviolet and visible regions and up to about 14 μm in the infrared. Typically, effective bandwidths are about 1.5% of the wavelength at peak transmittance, although this figure is reduced to 0.15% in some narrow-band filters; these have maximum transmittances of 10%.

Interference Wedges

An interference wedge consists of a pair of mirrored, partially transparent plates separated by a wedge-shaped layer of a dielectric material. The length of the plates ranges from about 50 to 200 mm. The radiation transmitted varies continuously in wavelength from one end to the other as the thickness of the wedge varies. By choosing the proper linear position along the wedge, a bandwidth of about 20 nm can be isolated.

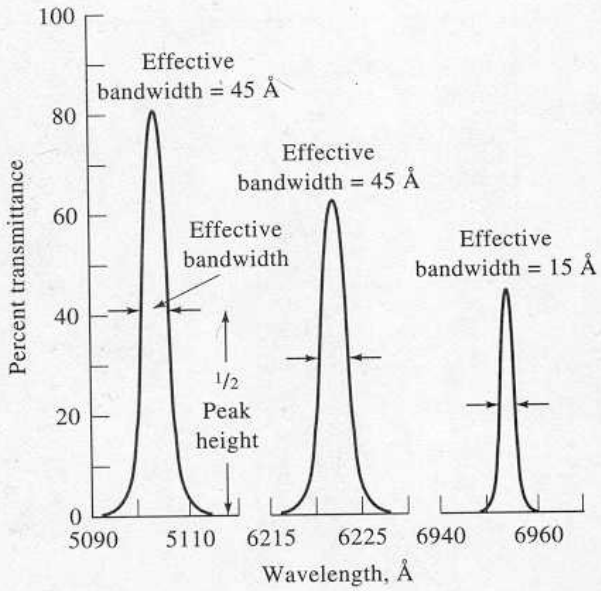

Figure 7-13 Transmission characteristics of typical interference filters.

Interference wedges are available for the visible region (400 to 700 nm), the near-infrared region (1000 to 2000 nm), and for several parts of the infrared region (2.5 to 14.5 μm). They can serve in place of prisms or gratings in monochromators.

Absorption Filters

Absorption filters, which are generally less expensive than interference filters, have been widely used for band selection in the visible region. These filters function by absorbing certain portions of the spectrum. The most common type consists of colored glass or of a dye suspended in gelatin and sandwiched between glass plates. The former have the advantage of greater thermal stability.

Absorption filters have effective bandwidths that range from perhaps 30 to 250 nm (see Figures 7-14 and 7-15). Filters that provide the narrowest bandwidths also absorb a significant fraction of the desired radiation and may have a transmittance of 10% or less at their band peaks. Glass filters with transmittance maxima throughout the entire visible region are available commercially.

Cut-off filters have transmittances of nearly 100% over a portion of the visible spectrum, but then rapidly decrease to zero transmittance over the remainder. A

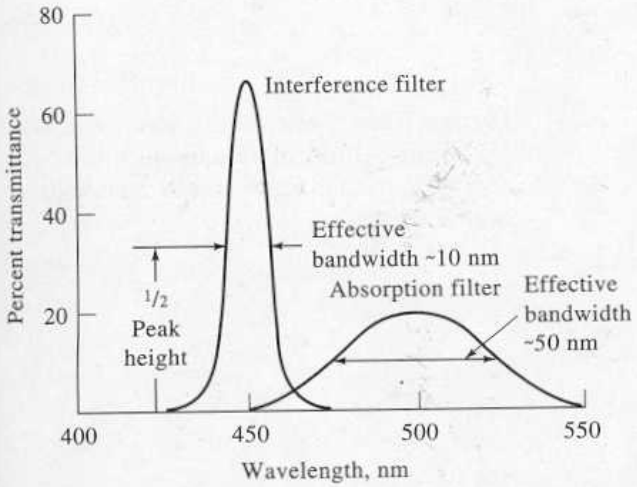

Figure 7-14 Effective bandwidths for two types of filters.

narrow spectral band can be isolated by coupling a cut-off filter with a second filter (see Figure 7-15).

It is apparent from Figure 7-14 that the performance characteristics of absorption filters are significantly inferior to those of interference-type filters. Not only are the bandwidths of absorption filters greater, but for narrow bandwidths the fraction of light transmitted is also less. Nevertheless, absorption filters are totally adequate for many applications.

7C-2 Monochromators

For many spectroscopic methods, it is necessary or desirable to be able to vary the wavelength of radiation continuously over a considerable range. This process is called *scanning* a spectrum. Monochromators are designed for spectral scanning. Monochromators for ultraviolet, visible, and infrared radiation are all similar in mechanical construction in the sense that they employ slits, lenses, mirrors, windows, and gratings or prisms. To be sure, the materials from which these components are fabricated depend upon the wavelength region of intended use (see Figure 7-2).

Components of Monochromators

Figure 7-16 illustrates the optical elements found in all monochromators, which include the following: (1) an entrance slit that provides a rectangular optical image, (2) a collimating lens or mirror that produces a parallel beam of radiation, (3) a prism or a grating that disperses the radiation into its component wavelengths, (4) a focusing element that reforms the image of the entrance slit and focuses it on a planar surface called a *focal plane,* and (5) an exit slit in the focal plane that isolates the desired spectral band. In addition, most monochromators have entrance and exit windows, which are designed to protect the components from dust and corrosive laboratory fumes.

As shown in Figure 7-16, two types of dispersing elements are found in monochromators: reflection gratings and prisms. For purposes of illustration, a beam made up of just two wavelengths, λ_1 and λ_2 ($\lambda_1 > \lambda_2$), is shown. This radiation enters the monochromators via a narrow rectangular opening or *slit,* is collimated, and then strikes the surface of the dispersing element at an angle. For the grating monochromator, angular dispersion of the wavelengths results from diffraction, which occurs at the reflective surface; for the prism, refraction at the two faces results in angular dispersal of the radiation, as shown. In both designs, the dispersed radiation is focused on the focal plane *AB* where it appears as two rectangular images of the entrance slit (one for λ_1 and one for λ_2). By rotating the dispersing element, one band or the other can be focused on the exit slit.

Historically, most monochromators were prism instruments. Currently, however, nearly all commercial monochromators are based upon reflection gratings because they are cheaper to fabricate, provide better wavelength separation for the same size dispersing element, and disperse radiation linearly along the focal plane. As shown in Figure 7-17a, linear dispersion means that the position of a band along the focal plane for a grating varies linearly with its wavelength. For prism instruments, in contrast, shorter wavelengths are

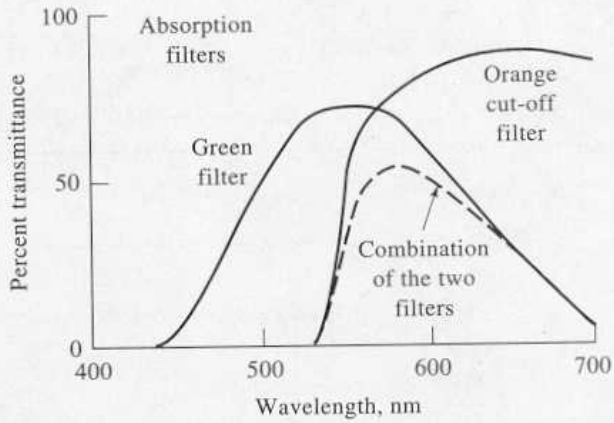

Figure 7-15 Comparison of various types of filters for visible radiation.

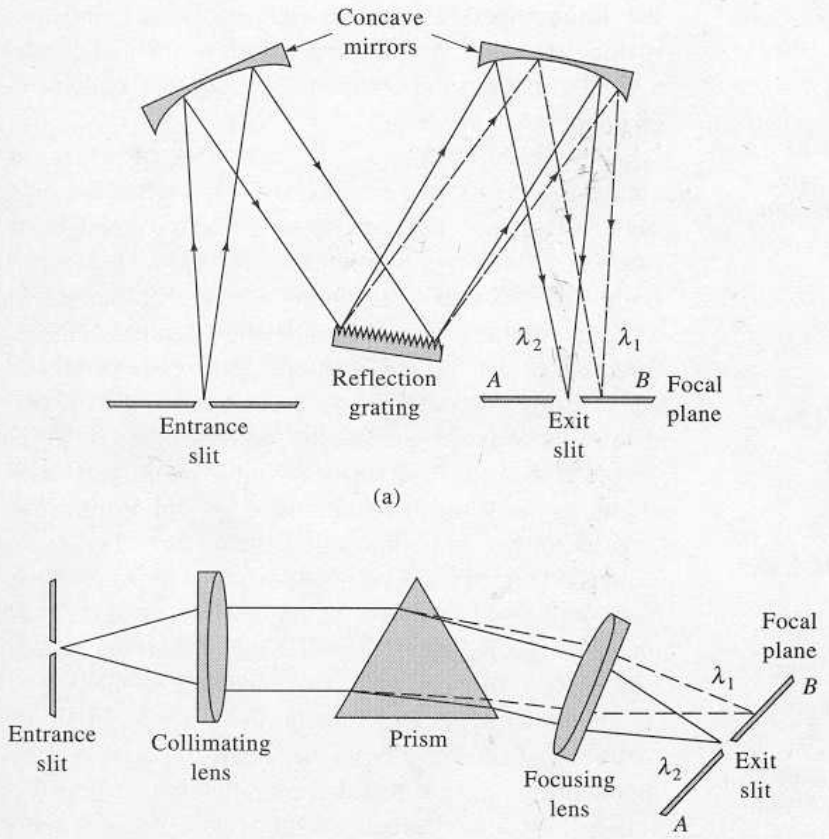

Figure 7-16 Two types of monochromators: (a) Czerney-Turner grating monochromator and (b) Bunsen prism monochromator. (In both instances, $\lambda_1 > \lambda_2$.)

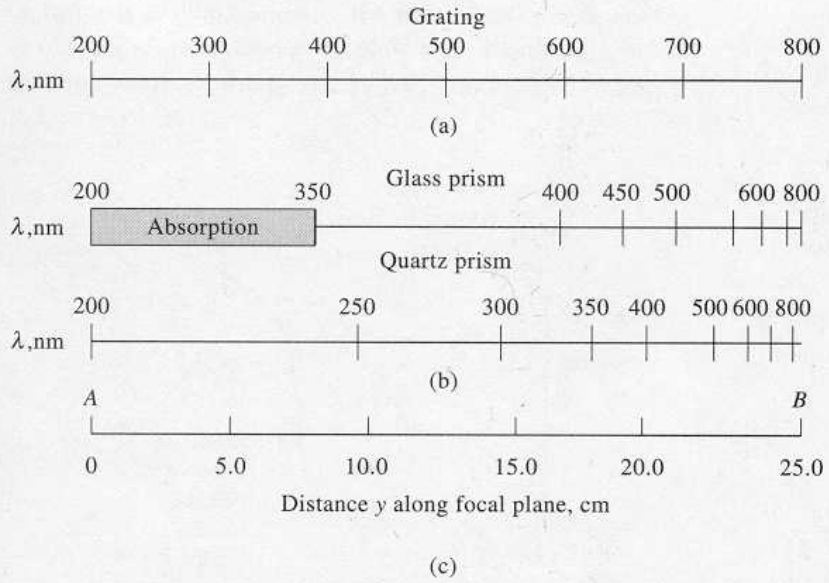

Figure 7-17 Dispersion for three types of monochromators. The points *A* and *B* on the scale in (c) correspond to the points shown in Figure 7-16.

dispersed to a greater degree than are longer ones, which complicates instrument design. The nonlinear dispersion of two types of prism monochromators is illustrated by Figure 7-17b. Because of their more general use, we will largely focus our discussion on grating monochromators.

Prism Monochromators

Prisms can be used to disperse ultraviolet, visible, and infrared radiation. The material used for their construction differs, however, depending upon the wavelength region (see Figure 7-2b).

Figure 7-18 shows the two most common types of prism designs. The first is a 60-deg prism, which is ordinarily fabricated from a single block of material. When crystalline (but not fused) quartz is the construction material, however, the prism is usually formed by cementing two 30-deg prisms together, as shown in Figure 7-18a; one is fabricated from right-handed quartz and the second from left-handed quartz. In this way, the optically active quartz causes no net polarization of the emitted radiation; this type of prism is called a *Cornu prism.* Figure 7-16b shows a *Bunsen monochromator,* which employs a 60-deg prism, likewise often made of quartz.

As shown in Figure 7-18b, the *Littrow prism,* which permits more compact monochromator designs, is a 30-deg prism with a mirrored back. Refraction in this type of prism takes place twice at the same interface so that the performance characteristics are similar to those of a 60-deg prism in a Bunsen mount.

Grating Monochromators

Dispersion of ultraviolet, visible, and infrared radiation can be brought about by directing a polychromatic beam through a *transmission grating* or onto the surface of a *reflection grating;* the latter is by far the more common type. *Replica gratings,* which are used in most monochromators are manufactured from a *master grating.*[13] The latter consists of a hard, optically flat, polished surface upon which have been ruled with a suitably shaped diamond tool a large number of parallel and closely spaced grooves. A magnified cross-sectional view of a few typical grooves is shown in Figure 7-19. A grating for the ultraviolet and visible region will typically contain from 300 to 2000 grooves/mm, with 1200 to 1400 being most common. For the infrared region, 10 to 200 grooves/mm are encountered; for spectrophotometers designed for the most widely used infrared range of 5 to 15 μm, a grating with about 100 grooves/mm is suitable. The construction of good master grating is tedious, time consuming, and expensive because the grooves must be identical in size, exactly parallel, and equally spaced over the length of the grating (3 to 10 cm).

Replica gratings are formed from a master grating by a liquid resin casting process that preserves virtually perfectly the optical accuracy of the original master grating on a clear resin surface. This surface is ordinarily made reflective by a coating of aluminum, or sometimes gold or platinum.

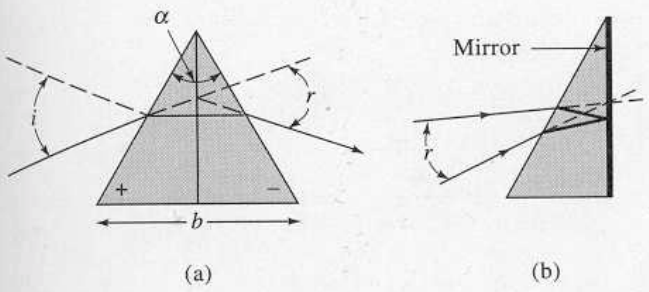

Figure 7-18 Dispersion by a prism: (a) quartz Cornu types and (b) Littrow type.

The Echellette Grating. Figure 7-19 is a schematic representation of an *echellette-type* grating, which is grooved or *blazed* such that it has relatively broad faces from which reflection occurs and narrow unused faces. This geometry provides highly efficient diffraction of radiation. Each of the broad faces can be considered to be a point source of radiation; thus interference among the reflected beams 1, 2, and 3 can occur. In order for the interference to be constructive, it is necessary that the path lengths differ by an integral multiple **n** of the wavelength λ of the incident beam.

In Figure 7-19, parallel beams of monochromatic radiation 1 and 2 are shown striking the grating at an incident angle *i* to the *grating normal.* Maximum constructive interference is shown as occurring at the reflected angle *r.* It is evident that beam 2 travels a greater distance than beam 1 and the difference in the paths is

[13] For an interesting and informative discussion of the manufacture, testing, and performance characteristics of gratings, see *Diffraction Grating Handbook,* Rochester, NY: Bausch and Lomb, Inc. (now Milton Roy Company), 1970. For a historical perspective on the importance of gratings in the advancement of science, see A. G. Ingalls, *Sci. Amer.,* **1952,** *186*(6), 45.

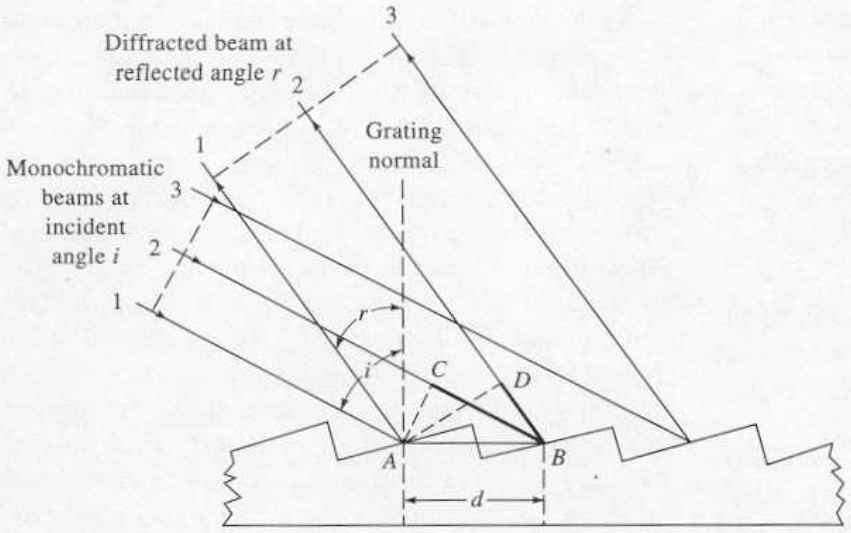

Figure 7-19 Mechanisms of diffraction from an echellette-type grating.

equal to $(\overline{CB} + \overline{BD})$ (shown as a broader line in the figure). For constructive interference to occur, this difference must equal $\mathbf{n}\lambda$. That is,

$$\mathbf{n}\lambda = (\overline{CB} + \overline{BD})$$

where **n,** a small whole number, is called the diffraction *order.* Note, however, that angle *CAB* is equal to angle *i* and that angle *DAB* is identical to angle *r.* Therefore, from simple trigonometry, we may write

$$\overline{CB} = d \sin i$$

where *d* is the spacing between the reflecting surfaces. It is also seen that

$$\overline{BD} = d \sin r$$

Substitution of the last two expressions into the first gives the condition for constructive interference. Thus,

$$\mathbf{n}\lambda = d(\sin i + \sin r) \qquad (7\text{-}6)$$

Equation 7-6 suggests that several values of λ exist for a given diffraction angle *r.* Thus, if a first-order line ($\mathbf{n} = 1$) of 900 nm is found at *r,* second-order (450-nm) and third-order (300-nm) lines also appear at this angle. Ordinarily, the first-order line is the most intense; indeed, it is possible to design gratings that concentrate as much as 90% of the incident intensity in this order. The higher-order lines can generally be removed by filters. For example, glass, which absorbs radiation below 350 nm, eliminates the higher-order spectra associated with first-order radiation in most of the visible region. The example that follows illustrates these points.

EXAMPLE 7-1

An echellette grating that contains 1450 blazes/mm was irradiated with a polychromatic beam at an incident angle 48 deg to the grating normal. Calculate the wavelengths of radiation that would appear at an angle of reflection of +20, +10, and 0 deg (angle *r,* Figure 7-19).

To obtain *d* in Equation 7-6, we write

$$d = \frac{1 \text{ mm}}{1450 \text{ blazes}} \times 10^6 \frac{\text{nm}}{\text{mm}} = 689.7 \frac{\text{nm}}{\text{blaze}}$$

When *r* in Figure 7-19 equals +20 deg,

$$\lambda = \frac{689.7}{\mathbf{n}} \text{ nm } (\sin 48 + \sin 20) = \frac{748.4}{\mathbf{n}} \text{ nm}$$

and the wavelengths for the first-, second-, and third-order reflections are 748, 374, and 249 nm, respectively.

Further calculations of a similar kind yield the following data:

	Wavelength (nm) for		
r, deg	n = 1	n = 2	n = 3
20	748	374	249
10	632	316	211
0	513	256	171

Concave Gratings. Gratings can be formed on a concave surface in much the same way as on a plane surface. A concave grating permits the design of a monochromator without auxiliary collimating and focusing mirrors or lenses because the concave surface both disperses the radiation and focuses it on the exit slit. Such an arrangement is advantageous in terms of cost; in addition, the reduction in number of optical surfaces increases the energy throughput of a monochromator that contains a concave grating.

Holographic Gratings.[14] One of the products from the emergence of laser technology is an optical (rather than mechanical) technique for forming gratings on plane or concave glass surfaces. *Holographic gratings* produced in this way are appearing in ever-increasing numbers in modern optical instruments, even some of the less expensive ones. Holographic gratings, because of their greater perfection with respect to line shape and dimensions, provide spectra that are freer from stray radiation and ghosts (double images).

In the preparation of holographic gratings, the beams from a pair of identical lasers are brought to bear at suitable angles upon a glass surface coated with photoresist. The resulting interference fringes from the two beams sensitize the photoresist so that it can be dissolved away, leaving a grooved structure that can be coated with aluminum or other reflecting substance to produce a reflection grating. The spacing of the grooves can be altered by changing the angle of the two laser beams with respect to one another. Nearly perfect, large (~50 cm) gratings with as many as 6000 lines/mm can be manufactured in this way at a relatively low cost. As with ruled gratings, replica gratings can be cast from a master holographic grating. It has been reported that no optical test exists that can distinguish between a master and replica holographic grating.[15]

Performance Characteristics of Grating Monochromators

The quality of a monochromator is dependent upon the purity of its radiant output, its ability to resolve adjacent wavelengths, its light-gathering power, and its spectral bandwidth. The last property is discussed in Section 7C-3.

Spectral Purity. The exit beam of a monochromator is usually contaminated with small amounts of scattered or stray radiation with wavelengths far different from that of the instrument setting. This unwanted radiation can be traced to several sources. Among these sources are reflections of the beam from various optical parts and the monochromator housing; the former arise from mechanical imperfections, particularly in gratings, introduced during manufacture. Scattering by dust particles in the atmosphere or on the surfaces of optical parts also causes stray radiation to reach the exit slit. Generally, the effects of spurious radiation are minimized by introducing baffles in appropriate spots in the monochromator and by coating interior surfaces with flat black paint. In addition, the monochromator is sealed with windows over the slits to prevent entrance of dust and fumes. Despite these precautions, however, some spurious radiation is still emitted; we shall see that its presence can have serious effects on absorption measurements under certain conditions.[16]

Dispersion of Grating Monochromators. The ability of a monochromator to separate different wavelengths is dependent upon its *dispersion.* The *angular dispersion* is given by $dr/d\lambda$ where dr is the change in the angle of reflection or refraction with a change in wavelength $d\lambda$. The angle r is defined in Figures 7-18 and 7-19.

The angular dispersion of a grating can be obtained by differentiating Equation 7-6 while holding i constant. Thus at any given angle of incidence,

$$\frac{dr}{d\lambda} = \frac{\mathbf{n}}{d \cos r} \tag{7-7}$$

The *linear dispersion* D refers to the variation in wavelength as a function of y, the distance along the line AB of the focal planes as shown in Figure 7-16. If F is the focal length of the monochromator, the linear dispersion can be related to the angular dispersion by the relationship

$$D = \frac{dy}{d\lambda} = \frac{F dr}{d\lambda} \tag{7-8}$$

[14] See J. Flamand, A. Grillo, and G. Hayat, *Amer. Lab.*, **1975**, *7* (5), 47; and J. M. Lerner et al., *Proc. Photo-Opt. Instrum. Eng.*, **1980**, *240*, 72, 82.

[15] I. R. Altelmose, *J. Chem. Educ.*, **1986**, *63*, A221.

[16] For discussion of the detection, the measurement, and the effects of stray radiation, see W. Kaye, *Anal. Chem.*, **1981**, *53*, 2201; M. R. Sharpe, *Anal. Chem.*, **1984**, *56*, 339A.

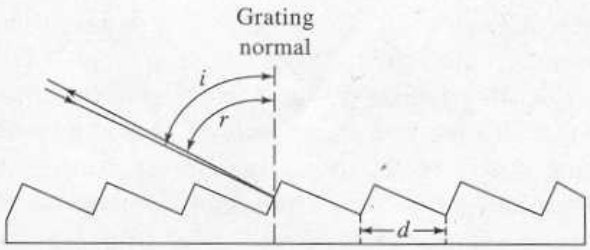

Figure 7-20 Echelle grating: i = angle of incidence; r = angle of reflection; d = groove spacing. In usual practice, $i \approx r = \beta = 63°26'$.

A more useful measure of dispersion is the *reciprocal linear dispersion* D^{-1} where

$$D^{-1} = \frac{d\lambda}{dy} = \frac{1}{F}\frac{d\lambda}{dr} \tag{7-9}$$

The dimensions of D^{-1} are often nm/mm or Å/mm.

Substitution of Equation 7-7 into Equation 7-9 leads to the reciprocal linear dispersion for a grating monochromator:

$$D^{-1} = \frac{d\lambda}{dy} = \frac{d \cos r}{\mathbf{n}F} \tag{7-10}$$

Note that the angular dispersion increases as the distance d between rulings decreases or as the number of lines per millimeter increases. At small angles of diffraction (<20 deg) cos $r \approx 1$, and Equation 7-10 becomes approximately

$$D^{-1} = \frac{d}{\mathbf{n}F} \tag{7-11}$$

Note that, for all practical purposes, if the angle r is small, the *linear dispersion of a grating monochromator is constant,* a property that greatly simplifies monochromator design.

Resolving Power of Monochromators The *resolving power* R of a monochromator describes the limit of its ability to separate adjacent images that have a slight difference in wavelength. Here, by definition

$$R = \lambda/\Delta\lambda \tag{7-12}$$

where λ is the average wavelength of the two images and $\Delta\lambda$ is their difference. The resolving power of typical bench-top ultraviolet/visible monochromators ranges from 10^3 to 10^4.

It can be shown[17] that the resolving power of a grating is given by the expression

$$R = \frac{\lambda}{\Delta\lambda} = \mathbf{n}N \tag{7-13}$$

when **n** is the diffraction order and N is the number of grating blazes illuminated by radiation from the entrance slit. Thus, better resolution is a characteristic of longer gratings, smaller blaze spacings, and higher diffraction orders. This equation applies to both echellette and echelle gratings.

Light-Gathering Power of Monochromators. In order to increase the signal-to-noise ratio of a spectrometer, it is necessary that the radiant energy that reaches the detector must be as large as possible. The *f/number* or *speed* provides a measure of the ability of a monochromator to collect the radiation that emerges from the entrance slit. The *f*/number is defined by the equation

$$f = F/d \tag{7-14}$$

where F is the focal length of the collimating mirror (or lens) and d is its diameter. The light-gathering power of an optical device increases as the inverse square of the *f*/number. Thus, an *f*/2 lens gathers four times more light than an *f*/4 lens. The *f*/numbers for many monochromators lie in the 1 to 10 range.

Echelle Monochromators. Echelle monochromators contain two dispersing elements arranged in series. The first of these elements is a special type of grating called an *echelle grating.* The second, which follows, is usually a low-dispersion prism, or sometimes a grating. The echelle grating, which was first described by G. R. Harrison in 1949, provides higher dispersion and higher resolution than an echellette of the same size.[18] Figure 7-20 shows a cross section of a typical echelle grating. It differs from the echellette grating shown in Figure 7-19 in several respects. First, in order to achieve a high angle of incidence, the blaze angle of an echelle grating is significantly greater than the conventional device, and the short side of the blaze is used rather than the long. Fur-

[17] R. A. Sawyer, *Experimental Spectroscopy,* 2nd ed., p. 130. Englewood Cliffs, NJ: Prentice Hall, 1951.

[18] For a more detailed discussion of the echelle grating, see P. N. Keliher and C. C. Wohlers, *Anal. Chem.,* **1976**, *48*, 333A; D. L. Anderson, A. R. Forster, and M. L. Parsons, *Anal. Chem.,* **1981**, *53*, 770; A. T. Zander and P. N. Keliher, *Appl. Spectrosc.,* **1979**, *33*, 499.

thermore the grating is relatively coarse, having typically 300 or fewer grooves per millimeter for ultraviolet/visible radiation. Note that the angle of refraction r is much higher in the echelle grating than the echellette and approaches the angle of incidence i. That is,

$$r \approx i = \beta$$

Under these circumstances, Equation 7-6 for a grating becomes

$$\mathbf{n}\lambda = 2d \sin \beta \qquad (7\text{-}15)$$

With a normal echellette grating, high dispersion, or low reciprocal dispersion, is obtained by making the groove width d small and the focal length F large. A large focal length reduces light gathering and makes the monochromator large and unwieldy. In contrast, the echelle grating achieves high dispersion by making both the angle β and the order of diffraction **n** large. The reciprocal dispersion for an echelle grating can then be obtained by modifying Equation 7-10 to

$$D^{-1} = \frac{2d \cos \beta}{\mathbf{n}F} \qquad (7\text{-}16)$$

The advantages of the echelle grating are illustrated by the data in Table 7-1, which show the performance characteristics for two typical monochromators, one with a conventional echellette grating and the other with an echelle. Note that for the same focal length the linear dispersion and resolution are an order of magnitude greater for the echelle; the light-gathering power of the echelle is also somewhat superior.

TABLE 7-1 Comparison of Performance Characteristics of a Conventional and Echelle Monochromator*

	Conventional	Echelle
Focal length	0.5 m	0.5 m
Groove density	1200/mm	79/mm
Diffraction angle, β	10°22′	63°26′
Order **n** (at 300 nm)	1	75
Resolution (at 300 nm), $\lambda/\Delta\lambda$	62,400	763,000
Reciprocal linear dispersion, D^{-1}	16 Å/mm	1.5 Å/mm
Light-gathering power, f	*f*/9.8	*f*/8.8

*With permission from P. E. Keliher and C. C. Wohlers, *Anal. Chem.*, **1976**, *48*, 334A. Copyright 1976 American Chemical Society.

One of the problems encountered with the use of an echelle grating is that the linear dispersion at high orders of refraction is so great that to cover a reasonably broad spectral range it is necessary to use many successive orders. For example, one instrument designed to cover a range of 200 to 800 nm employs diffraction orders 28 to 118 (90 successive orders). Because these orders inevitably overlap, it is essential that a system of cross dispersion, such as that shown in Figure 7-21a, be employed with an echelle grating. Here, the dispersed radiation from the grating is passed through a prism (in some systems, a second grating is used) whose axis is at 90 deg to the grating. The effect of this arrangement is to produce a two-dimensional spectrum as shown schematically in Figure 7-21b. In this figure, the locations of 8 of the 70 orders is indicated by short vertical lines. For any given order, the wavelength dispersion is approximately linear, but, as can be seen, the dispersion lessens at lower orders or higher wavelengths. An actual two-dimensional spectrum from an echelle monochromator consists of a complex series of short vertical lines lying along 50 to 100 horizontal axes, each axis corresponding to one diffraction order. To change wavelength with an echelle monochromator, it is necessary to change the angle of both the grating and the prism.

Recently, several instrument manufacturers have begun to offer echelle-type spectrometers for simultaneous determination of a multitude of elements by atomic emission spectroscopy. The optical designs of two of these instruments are shown in Figures 10-7 and 10-9.

7C-3 Monochromator Slits

The slits of a monochromator play an important role in determining the monochromator's performance characteristics and quality. Slit jaws are formed by carefully machining two pieces of metal to give sharp edges. Care is taken to assure that the edges of the slit are exactly parallel to one another and that they lie on the same plane. In some monochromators, the openings of the two slits are fixed; more commonly, the spacing can be adjusted with a micrometer mechanism.

The entrance slit (see Figure 7-16) of a monochromator serves as a radiation source; its image is ultimately focused on the focal plane that contains the exit slit. If the radiation source consists of a few discrete

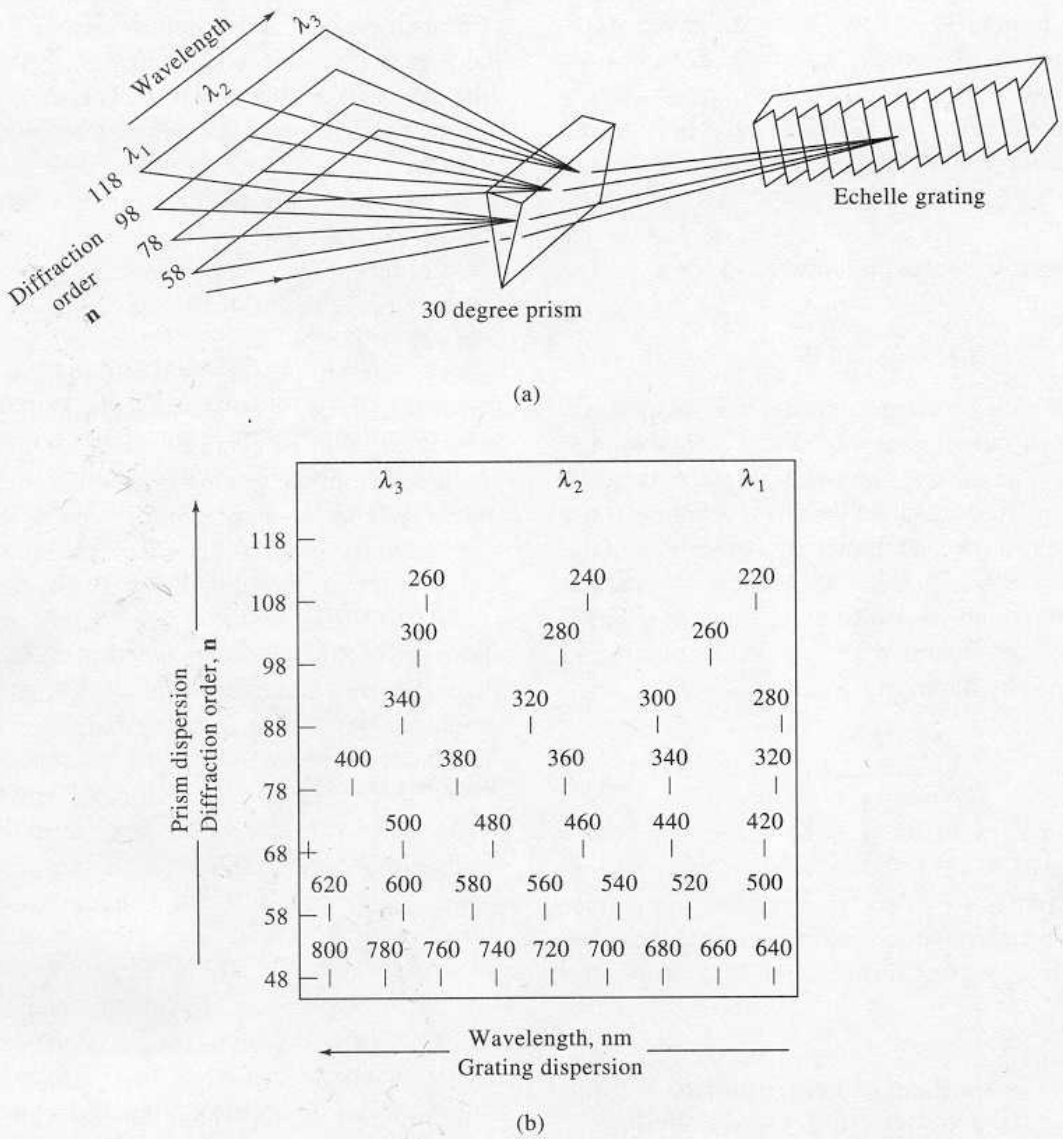

Figure 7-21 An echelle monochromator: (a) arrangement of dispersing elements, and (b) schematic end-on view of the dispersed radiation from the point of view of the transducer.

wavelengths, a series of rectangular images appears on this surface as bright lines, each corresponding to a given wavelength. A particular line can be brought to focus on the exit slit by rotating the dispersing element. If the entrance and exit slits are of the same size (as is usually the case), the image of the entrance slit will in theory just fill the exit-slit opening when the setting of the monochromator corresponds to the wavelength of the radiation. Movement of the monochromator mount in one direction or the other results in a continuous decrease in emitted intensity, zero being reached when the entrance-slit image has been displaced by its full width.

Effect of Slit Width on Resolution

Figure 7-22 illustrates the situation in which monochromatic radiation of wavelength λ_2 strikes the exit slit. Here, the monochromator is set for λ_2 and the two slits are identical in width. The image of the entrance slit just fills the exit slit. Movement of the monochromator to a setting of λ_1 or λ_3 results in the image being moved completely out of the slit. The lower half of Figure 7-22 shows a plot of the radiant power emitted as a function of monochromator setting. Note that the *bandwidth* is defined as the span of monochromator settings (in units of wavelength, or sometimes in units of cm^{-1}) needed

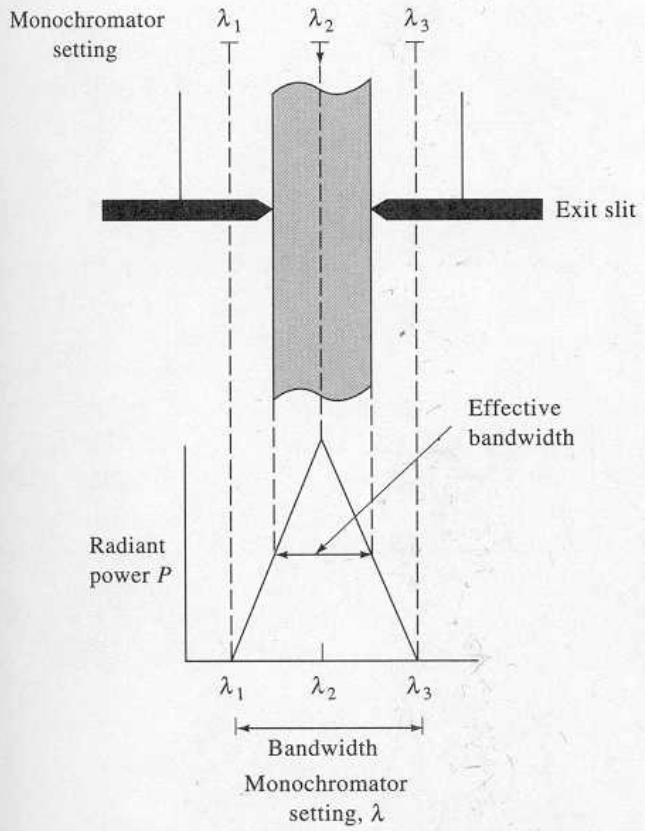

Figure 7-22 Illumination of an exit slit by monochromatic radiation λ_2 at various monochromator settings. Exit and entrance slits are identical.

to move the image of the entrance slit across the exit slit. If polychromatic radiation were employed, it would also represent the span of wavelengths from the exit slit for a given monochromator setting.

The *effective bandwidth,* which is one half the bandwidth when the two slit widths are identical, is seen to be the range of wavelengths that exit the monochromator at a given wavelength setting. The effective bandwidth can be related to the reciprocal linear dispersion by writing Equation 7-8 in the form

$$D^{-1} = \frac{\Delta\lambda}{\Delta y}$$

where $\Delta\lambda$ and Δy are now finite intervals of wavelength and linear distance along the focal plane, respectively. As shown by Figure 7-22, when Δy is equal to the slit width w, $\Delta\lambda$ is the effective bandwidth. That is,

$$\Delta\lambda_{\text{eff}} = wD^{-1} \qquad (7\text{-}17)$$

Figure 7-23 illustrates the relationship between the effective bandwidth of an instrument and its ability to resolve spectral peaks. Here, the exit slit of a grating monochromator is illuminated with a beam composed of just three equally spaced lines at wavelengths, λ_1, λ_2, and λ_3; each line is assumed to be of the same intensity. In the top figure, the effective bandwidth of the instrument is exactly equal to the difference in wavelength between λ_1 and λ_2 or λ_2 and λ_3. When the monochromator is set at λ_2, radiation of this wavelength just fills the slit. Movement of the monochromator in either direction diminishes the transmitted intensity of λ_2, but increases the intensity of one of the other lines by an equivalent amount. As shown by the solid line in the plot to the right, no spectral resolution of the three wavelengths is achieved.

In the middle drawing of Figure 7-23, the effective bandwidth of the instrument has been reduced by narrowing the openings of the exit and entrance slits to three quarters that of their original dimensions. The solid line in the plot on the right shows that partial resolution of the three lines results. When the effective bandwidth is decreased to one half the difference in wavelengths of the three beams, complete resolution is achieved, as shown in the bottom drawing. Thus, complete resolution of two lines is feasible only if the slit width is adjusted so that the effective bandwidth of the monochromator is equal to one half the wavelength difference of the lines.

EXAMPLE 7-2

A grating monochromator with a reciprocal linear dispersion of 1.2 nm/mm is to be used to separate the sodium lines at 589.0 and 589.6. In theory, what slit width would be required?

Complete resolution of the two lines requires that

$$\Delta\lambda_{\text{eff}} = \frac{1}{2}(589.6 - 589.0) = 0.3 \text{ nm}$$

Substitution into Equation 7-15 after rearrangement gives

$$w = \frac{\Delta\lambda_{\text{eff}}}{D^{-1}} = \frac{0.3 \text{ nm}}{1.2 \text{ nm/mm}} = 0.25 \text{ mm}$$

It is important to note that slit widths calculated as in Example 7-2 are theoretical. Imperfections, which are present in most monochromators, are such that slit widths narrower than theoretical are usually required to achieve a desired resolution.

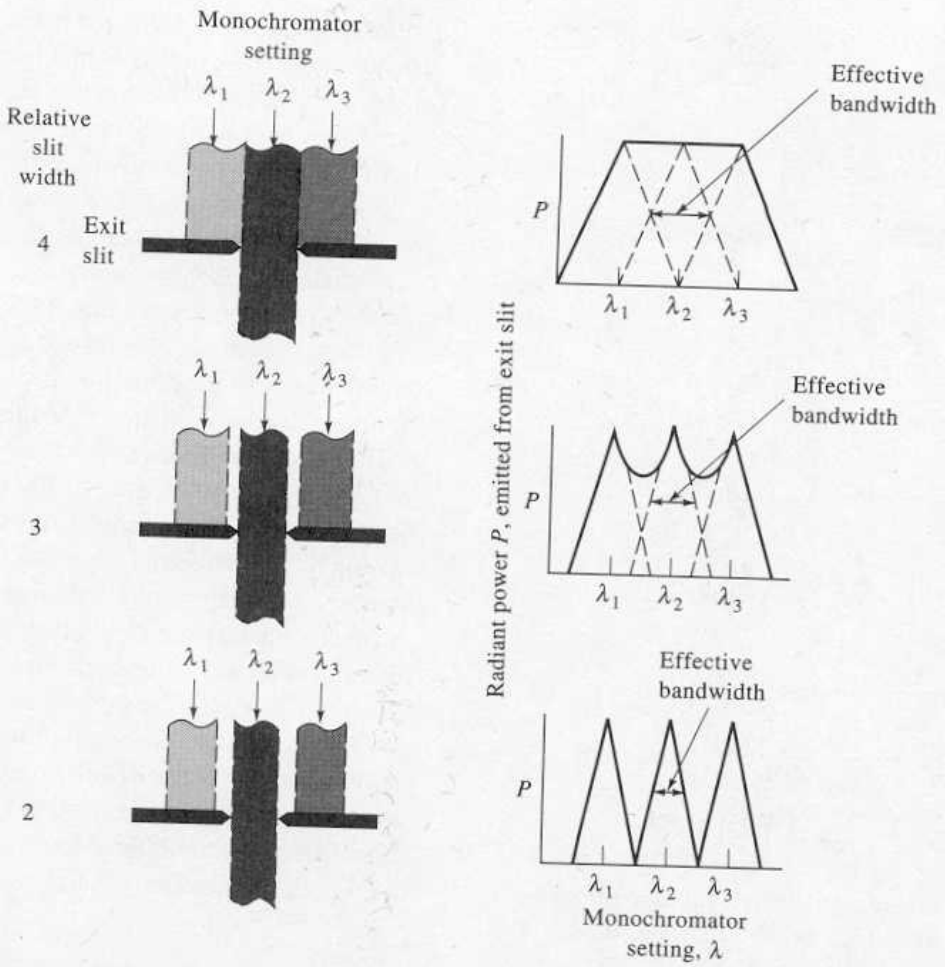

Figure 7-23 The effect of the slit width on spectra. The entrance slit is illuminated with λ_1, λ_2, and λ_3 only. Entrance and exit slits are identical. Plots on the right show changes in emitted power as the setting of monochromator is varied.

Figure 7-24 shows the effect of bandwidth on experimental spectra for benzene vapor. Note the much greater spectral detail realized with the narrowest slit setting and thus the narrowest bandwidth.

Choice of Slit Widths

The effective bandwidth of a monochromator depends upon the dispersion of the grating or prism as well as the width of the entrance and exit slits. Most monochromators are equipped with variable slits so that the effective bandwidth can be changed. The use of minimal slit width is desirable when the resolution of narrow absorption or emission bands is needed. On the other hand, a marked decrease in the available radiant power accompanies a narrowing of slits, and accurate measurement of this power becomes more difficult. Thus, wider slit widths may be used for quantitative analysis rather than for qualitative work, where spectral detail is important.

7D SAMPLE CONTAINERS

Sample containers are required for all spectroscopic studies except emission spectroscopy. In common with the optical elements of monochromators, the *cells* or *cuvettes* that hold the samples must be made of material that is transparent to radiation in the spectral region of interest. Thus, as shown in Figure 7-2, quartz or fused silica is required for work in the ultraviolet region (below 350 nm); both of these substances are transparent in the visible region and up to about 3 μm in the infrared region as well. Silicate glasses can be employed in the region between 350 and 2000 nm. Plastic containers have also found application in the visible region. Crystalline sodium chloride is the most common substance employed for cell windows in the infrared region; the other infrared transparent materials listed in Figure 7-2 may also be used for this purpose.

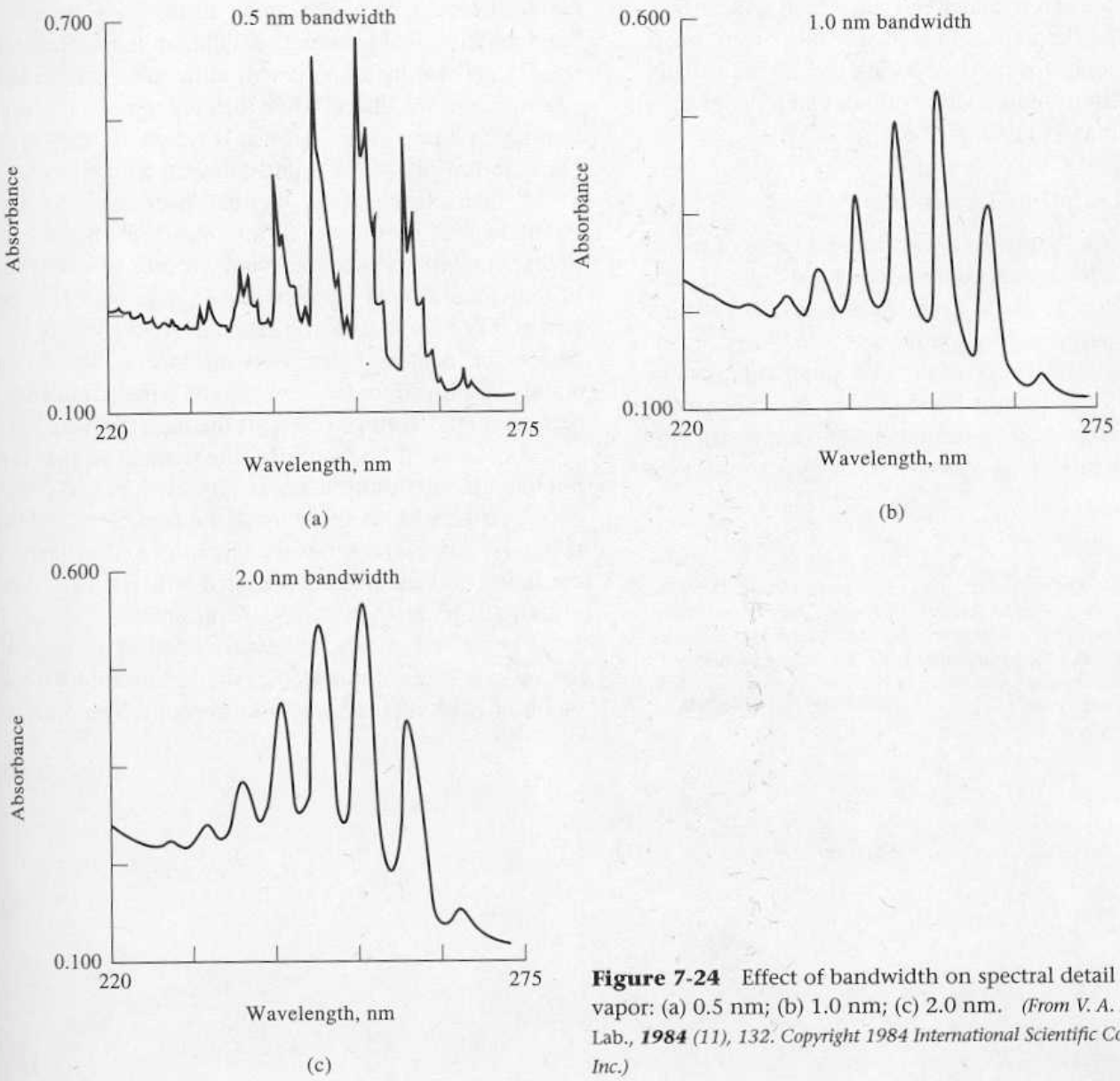

Figure 7-24 Effect of bandwidth on spectral detail for benzene vapor: (a) 0.5 nm; (b) 1.0 nm; (c) 2.0 nm. *(From V. A. Kohler,* Amer. Lab., ***1984*** *(11), 132. Copyright 1984 International Scientific Communications Inc.)*

7E RADIATION TRANSDUCERS

7E-1 Introduction

The detectors for early spectroscopic instruments were the human eye or a photographic plate or film. These detection devices have been largely supplanted by transducers that convert radiant energy into an electrical signal; our discussion will be largely confined to these more modern detectors.

Properties of the Ideal Transducer

The ideal transducer would have a high sensitivity, a high signal-to-noise ratio, and a constant response over a considerable range of wavelengths. In addition, it would exhibit a fast response time and a zero output signal in the absence of illumination. Finally, the electrical signal produced by the transducer would be directly proportional to the radiant power P. That is,

$$S = kP \tag{7-18}$$

where S is the electrical response in terms of current or voltage, and k is the calibration sensitivity (Section 1D-2).

Many real transducers exhibit a small, constant response, known as a *dark current,* in the absence of radiation. For these transducers , the response is described by the relationship

$$S = kP + k_d \tag{7-19}$$

where k_d represents the dark current, which is ordinarily constant over short measurement periods. Instruments with transducers that produce a dark current are usually equipped with a compensating circuit that reduces k_d to zero; Equation 7-18 then applies.

Types of Radiation Transducers[19]

As indicated in Figure 7-3b, two general types of radiation transducers are encountered; one responds to photons, the other to heat. All photon transducers (also called *photoelectric* or quantum detectors) have an active surface, which is capable of absorbing radiation. In some types, the absorbed energy causes emission of electrons and the development of a photocurrent. In others, the radiation promotes electrons into conduction bands; detection here is based on the resulting enhanced conductivity *(photoconduction)*. Photon transducers are used largely for measurement of ultraviolet, visible, and near-infrared radiation. When they are applied to radiation much longer than 3 μm in wavelength, they must be cooled to dry-ice or liquid-nitrogen temperatures to avoid interference from thermal background noise. Photoelectric transducers differ from heat transducers in that the formers' electrical signal results from a series of individual events (absorption of single photons), the probability of which can be described by the use of statistics. In contrast, thermal transducers, which are widely employed for the detection of infrared radiation, respond to the average power of the incident radiation.

As shown in Section 5B-2 the distinction between photon and heat transducers is important because shot noise often limits the behavior of the former while thermal noise frequently limits the latter. As a consequence, the indeterminate errors associated with the two types of transducers are fundamentally different.

Figure 7-25 shows the relative spectral response of the various kinds of transducers that are useful for ultraviolet, visible, and infrared spectroscopy. The ordinate

[19] For a discussion of optical radiation detectors, see E. L. Dereniak and D. G. Crowe, *Optical Radiation Detectors*. New York: Wiley, 1984; F. Grum and R. J. Becherer, *Optical Radiation Measurements*, Vol. 1. New York: Academic Press, 1979; J. D. Ingle Jr., and S. R. Crouch *Spectrochemical Analysis*, pp. 106–117. Englewood Cliffs, NJ: Prentice Hall, 1988.

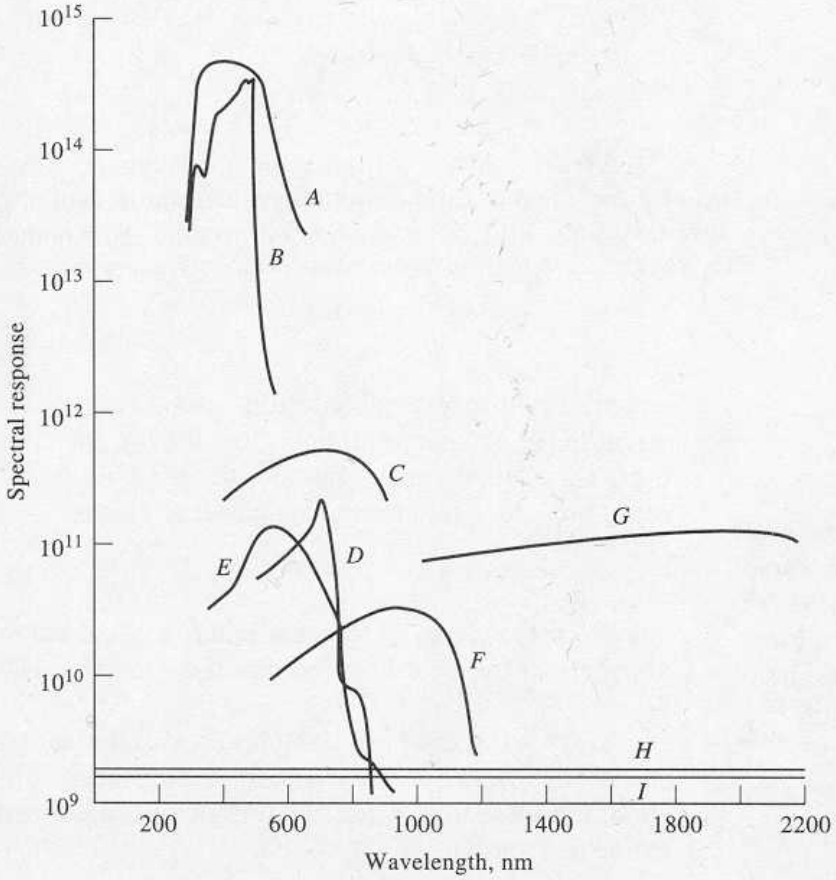

Figure 7-25 Relative response of various types of photoelectric transducers *(A–G)* and heat transducers *H, I*): *A,* photomultiplier tube; *B,* CdS photoconductivity; *C,* GaAs photovoltaic cell; *D,* CdSe photoconductivity cell; *E,* Se/SeO photovoltaic cell; *F,* silicon photodiode; *G,* PbS photoconductivity; *H,* thermocouple; *I,* Golay cell. *(Adapted from P. W. Druse, L. N. McGlauchlin, and R. B. Quistan,* Elements of Infrared Technology, *pp. 424–425. New York: Wiley, 1962. Reprinted by permission of John Wiley & Sons Inc.)*

function is inversely related to the noise of the transducers and directly related to the square root of its surface area. Note that the relative sensitivity of the thermal transducers (curves *H* and *I*) is independent of wavelength but significantly lower than the sensitivity of photoelectric transducers. On the other hand, photon transducers are often far from ideal with respect to constant response versus wavelength.

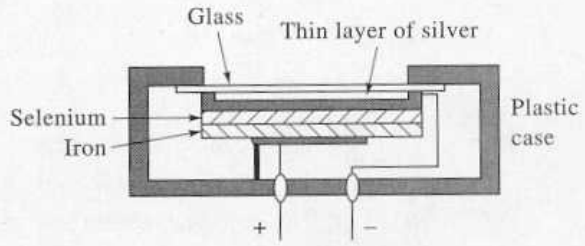

Figure 7-26 Schematic of a typical barrier-layer cell.

7E-2 Photon Transducers

Several types of photon transducers are available, including: (1) photovoltaic cells, in which the radiant energy generates a current at the interface of a semiconductor layer and a metal; (2) phototubes, in which radiation causes emission of electrons from a photosensitive solid surface; (3) photomultiplier tubes, which contain a photoemissive surface as well as several additional surfaces that emit a cascade of electrons when struck by electrons from the photosensitive area; (4) photoconductivity transducers in which absorption of radiation by a semiconductor produces electrons and holes, thus leading to enhanced conductivity; (5) silicon photodiodes, in which photons increase the conductance across a reverse-biased *pn* junction; and (6) charge-transfer transducers, in which the charges developed in a silicon crystal as a result of absorption of photons are collected and measured.[20]

Photovoltaic or Barrier-Layer Cells

The photovoltaic cell is a simple device that is used for detecting and measuring radiation in the visible region. The typical cell has a maximum sensitivity at about 550 nm; the response falls off to perhaps 10% of the maximum at 350 and 750 nm (see Figure 7-25*E*). Its range approximates that of the human eye.

The photovoltaic cell consists of a flat copper or iron electrode upon which is deposited a layer of semiconducting material, such as selenium (see Figure 7-26). The outer surface of the semiconductor is coated with a thin transparent metallic film of gold or silver, which serves as the second or collector electrode; the entire array is protected by a transparent envelope. When radiation of sufficient energy reaches the semiconductor, covalent bonds are broken, with the result that conduction electrons and holes are formed. The electrons then migrate toward the metallic film and the holes toward the base upon which the semiconductor is deposited. The liberated electrons are free to migrate through the external circuit to interact with these holes. The result is an electrical current of a magnitude that is proportional to the number of photons that strike the semiconductor surface. Ordinarily, the currents produced by a photovoltaic cell are large enough to be measured with a microammeter; if the resistance of the external circuit is kept small ($<400\ \Omega$), the photocurrent is directly proportional to the power of the radiation that strikes the cell. Currents on the order of 10 to 100 μA are typical.

The barrier-layer cell constitutes a rugged, low-cost means for measuring radiant power. No external source of electrical energy is required. On the other hand, the low internal resistance of the cell makes the amplification of its output less convenient. Consequently, although the barrier-layer cell provides a readily measured response at high levels of illumination, it suffers from lack of sensitivity at low levels. Another disadvantage of the barrier-type cell is that it exhibits *fatigue* in which its current output decreases gradually during continued illumination; proper circuit design and choice of experimental conditions minimize this effect. Barrier-type cells find use in simple, portable instruments where ruggedness and low cost are important. For routine analyses, these instruments often provide perfectly reliable analytical data.

Vacuum Phototubes[21]

A second type of photoelectric device is the vacuum phototube, which consists of a semicylindrical cathode and a wire anode sealed inside an evacuated transparent

[20] For a comparison of the performance characteristics of the three most sensitive and widely used photon transducers, namely photomultipliers, silicon diodes, and charge-transfer devices, see W. E. L. Grossman, *J. Chem. Educ.*, **1989**, *66*, 697.

[21] For a discussion of vacuum phototubes and photomultiplier tubes, see F. E. Lytle, *Anal. Chem.*, **1974**, *46*, 545A.

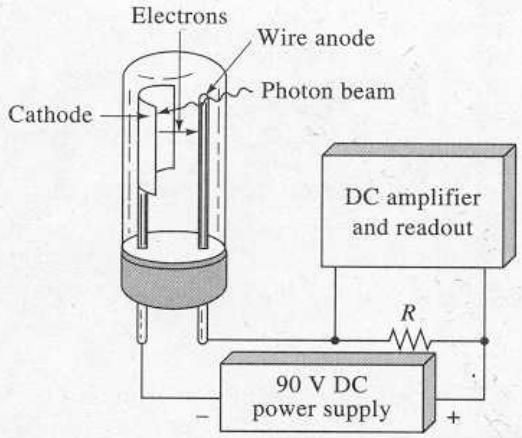

Figure 7-27 A phototube and accessory circuit. The photocurrent induced by the radiation causes a potential drop across *R*, which is then amplified to drive a meter or recorder.

envelope (see Figure 7-27). The concave surface of the electrode supports a layer of photoemissive material (Section 6C-1) that tends to emit electrons when it is irradiated. When a potential is applied across the electrodes, the emitted electrons flow to the wire anode generating a photocurrent that is generally about one tenth as great as that associated with a photovoltaic cell for a given radiant intensity. In contrast, however, amplification is easily accomplished since the phototube has a high electrical resistance.

The number of electrons ejected from a photoemissive surface is directly proportional to the radiant power of the beam that strikes that surface. As the potential applied across the two electrodes of the tube is increased, the fraction of the emitted electrons that reaches the anode rapidly increases; when the saturation potential is achieved, essentially all of the electrons are collected at the anode. The current then becomes independent of potential and directly proportional to the radiant power. Phototubes are usually operated at a potential of about 90 V, which is well within the saturation region.

A variety of photoemissive surfaces are used in commercial phototubes. Typical examples are shown in Figure 7-28. From the user's standpoint, photoemissive surfaces fall into four categories: highly sensitive, red sensitive, ultraviolet sensitive, and flat response. The most sensitive cathodes are bialkali types such as number 117 in Figure 7-28; they are made up of potassium, cesium, and antimony. Red-sensitive materials are multialkali types (for example, Na/K/Cs/Sb), or Ag/O/Cs formulations. The behavior of the latter is shown as S-11 in the figure. Compositions of Ga/In/As extend the red region up to about 1.1 μm. Most formulations are ultraviolet sensitive provided the tube is equipped with transparent windows. Flat responses are obtained with Ga/As compositions such as that labeled 128 in Figure 7-28.

Phototubes frequently produce a small dark current (see Equation 7-19) that results from thermally induced electron emission and natural radioactivity from ^{40}K in the glass housing of the tube.

Photomultiplier Tubes

For the measurement of low radiant power, the *photomultiplier tube* (PMT) offers advantages over the ordinary phototube.[22] Figure 7-29 is a schematic of such a device. The photo cathode surface is similar in composition to the surfaces of the phototubes described in Figure 7-28, and it emits electrons when exposed to radiation. The tube also contains additional electrodes (nine in Figure 7-29) called *dynodes*. Dynode 1 is maintained at a potential 90 V more positive than the cathode, and electrons are accelerated toward it as a consequence. Upon striking the dynode, each photoelectron causes emission of several additional electrons; these, in turn, are accelerated toward dynode 2, which is 90 V more positive than dynode 1. Again, several electrons are emitted for each electron that strikes the surface. By the

[22] For a detailed discussion of the theory and applications of photomultipliers, see R. W. Engstrom, *Photomultiplier Handbook*, Lancaster, PA: RCA Corporation, 1980.

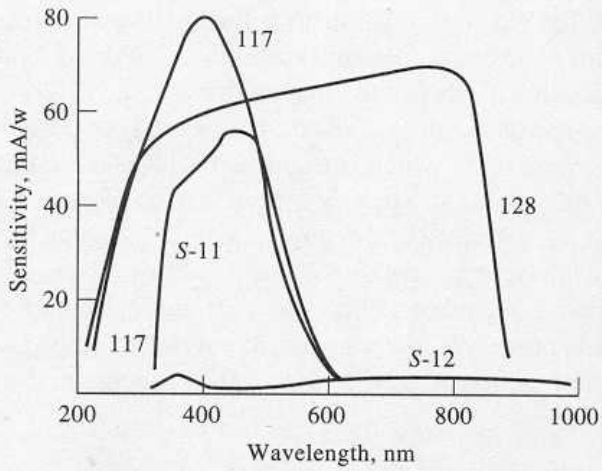

Figure 7-28 Spectral response of some typical photoemissive surfaces. *(From F. E. Lytle,* Anal. Chem., ***1974,*** *46, 546A. Copyright 1974 American Chemical Society.)*

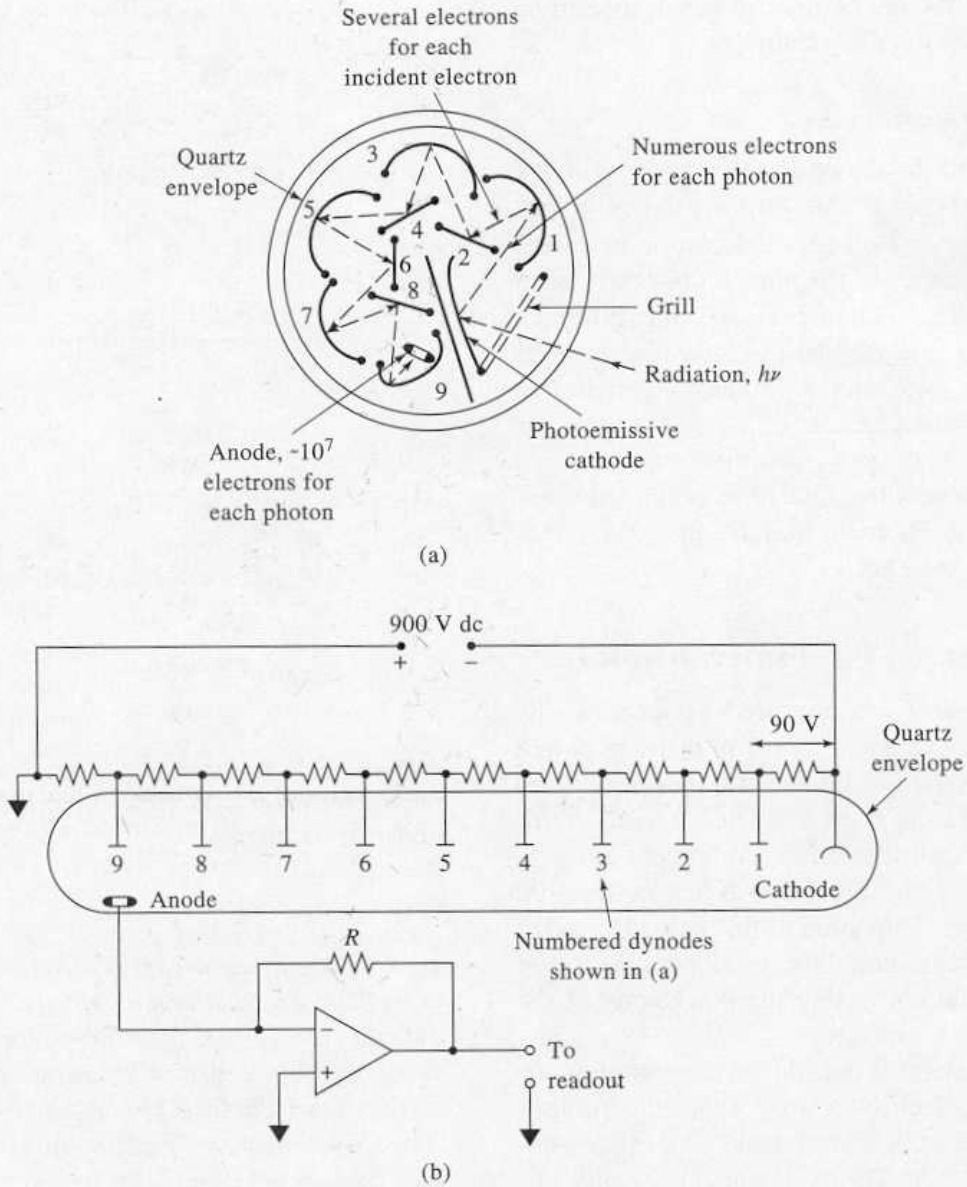

Figure 7-29 Photomultiplier tube: (a) cross-section of the tube and (b) electrical circuit.

time this process has been repeated nine times, 10^6 to 10^7 electrons have been formed for each incident photon; this cascade is finally collected at the anode and the resulting current is then electronically amplified and measured.

As shown by Figure 7-25*A*, photomultipliers are highly sensitive to ultraviolet and visible radiation; in addition, they have extremely fast time responses. Often, the sensitivity of an instrument with a photomultiplier is limited by its dark-current emission. Because thermal emission is the major source of dark-current electrons, the performance of a photomultiplier can be enhanced by cooling. In fact, thermal dark currents can be virtually eliminated by cooling the detector to −30°C. Transducer housings, which can be cooled by circulation of an appropriate coolant, are available commercially.

Photomultiplier tubes are limited to measuring low-power radiation because intense light causes irreversible damage to the photoelectric surface. For this reason, the device is always housed in a light-tight compartment, and care is taken to eliminate the possibility of its being exposed even momentarily to daylight or other strong light. With appropriate external circuitry,

photomultiplier tubes can be used to detect the arrival of a single photon at the photocathode.

Silicon Diode Transducers

A silicon diode transducer consists of a reverse-biased *pn* junction formed on a silicon chip. As shown in Figure 7-30, the reverse bias creates a depletion layer that reduces the conductance of the junction to nearly zero. If radiation is allowed to impinge on the chip, however, holes and electrons are formed in the depletion layer and swept through the device to produce a current that is proportional to radiant power.

Silicon diodes are more sensitive than vacuum phototubes but less sensitive than photomultiplier tubes (see Figure 7-25*F*). Photodiodes have spectral ranges from about 190 to 1100 nm.

7E-3 Multichannel Photon Transducers[23]

The first multichannel detector used in spectroscopy was a photographic plate or a film strip that was placed along the length of the focal plane of a spectrometer so that all the lines in a spectrum could be recorded simultaneously. Photographic detection is relatively sensitive with some emulsions that respond to as few as 10 to 100 photons. The primary limitation of this type of detector is, however, the time required for developing the image of the spectrum and converting the blackening of the emulsion to radiant intensities.

Modern multichannel transducers consist of an array of small photoelectric-sensitive elements arranged either linearly or in a two-dimensional pattern on a single semiconductor chip. The chip, which is usually silicon and typically has dimensions of a few millimeters on a side, also contains electronic circuitry that makes it possible to determine the electrical output signal from each of the photosensitive elements either sequentially or simultaneously. For spectroscopic studies, a multichannel transducer is generally placed in the focal plane of a spectrometer so that various elements of the dispersed spectrum can be transduced and measured simultaneously.

At the present time three types of multichannel devices are used in commercial spectroscopic instruments: *photodiode arrays* (PDAs), *charge-injection devices* (CIDs), and *charge-coupled devices* (CCDs). Photodiode arrays are one-dimensional transducers in which the photosensitive elements are arranged in a line on the transducer face. In contrast, the individual photosensitive elements of charge-injection and charge-coupled devices are usually formed as two-dimensional arrays. Charge-injection and charge-coupled transducers both function by collecting photogenerated charges in various areas of the transducer surface and then measuring the quantity of charge accumulated in a brief period. In both devices, the measurement is accomplished by transferring the charge from a collection area to a detection area. For this reason, the two types of transducers are sometimes called *charge-transfer devices* (CTDs). These devices have widespread use as image transducers for television applications and in astronomy.

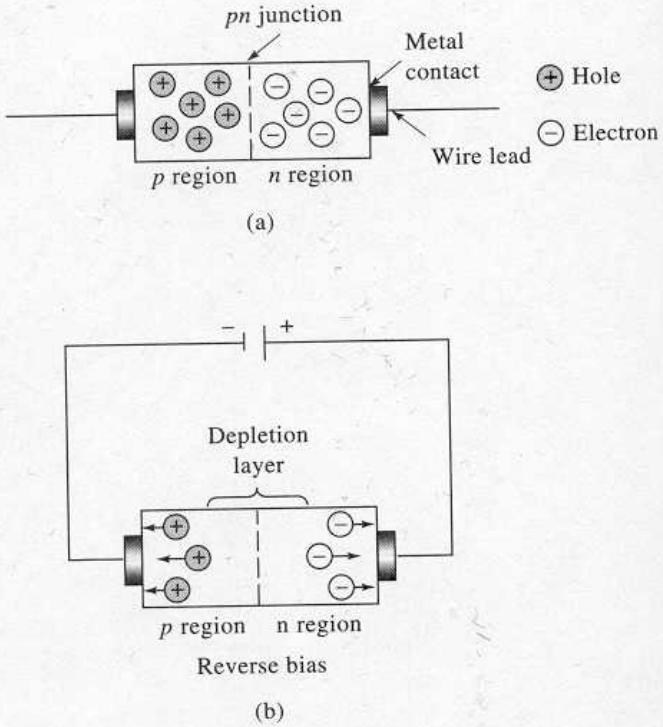

Figure 7-30 (a) Schematic of a silicon diode. (b) Formation of depletion layer, which prevents flow of electricity under reverse bias.

Photodiode Arrays

In a photodiode array, the individual photosensitive elements are small silicon photodiodes each of which consists of a reverse-biased *pn* junction (see previous section). The individual photodiodes are part of a

[23] For a discussion of multichannel photon detectors, see Y. Talmi, *Appl. Spectrosc.*, **1982**, *36*, 1; W. E. Grossman, *J. Chem. Educ.*, **1989**, *66*, 697; J. V. Sweedler, *Crit. Rev. Anal. Chem.*, **1993**, *24*, 59; D. G. Jones, *Anal. Chem.*, **1985**, *57*, 1057A.

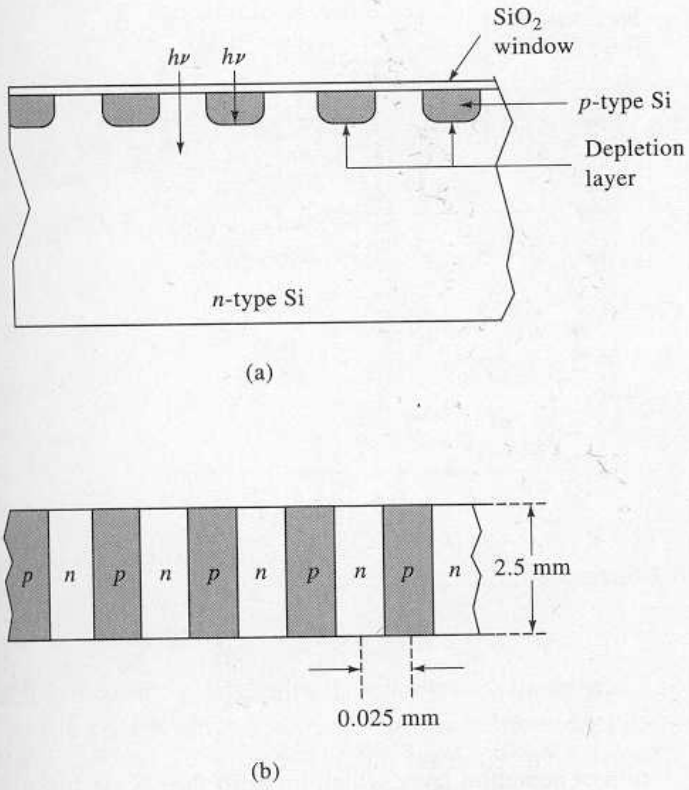

Figure 7-31 A reverse-biased linear diode-array detector: (a) cross section and (b) top view.

large-scale integrated circuit formed on a single silicon chip. Figure 7-31 shows the geometry of the surface region of a few of the transducer elements. Each element consists of a diffused *p*-type bar in an *n*-type silicon substrate to give a surface region that consists of a series of side-by-side elements that have typical dimensions of 2.5 by 0.025 mm (Figure 7-31b). Light that is incident upon these elements creates charges in both the *p* and *n* regions. The positive charges are collected and stored in the *p*-type bars for subsequent integration (the charges formed in the *n*-regions divide themselves proportionally between the two adjacent *p*-regions). The number of transducer elements in a chip ranges from 64 to 4096 with 1024 being perhaps the most widely used.

The integrated circuit that makes up a diode array also contains a storage capacitor and switch for each diode as well as a circuit for sequentially scanning the individual diode-capacitor circuits. Figure 7-32 is a simplified diagram that shows the arrangement of these components. Note that in parallel with each photodiode is a companion 10-pF storage capacitor. Each diode-capacitor pair is sequentially connected to a common output line by the N-bit shift register and the transistor switches. The shift register sequentially closes each of these switches momentarily causing the capacitor to be charged to −5 V, which then creates a reverse bias across the *pn* junction of the detector. Radiation that impinges upon the depletion layer in either the *p* or the *n* region forms charges (electrons and holes) that create a current that partially discharges the capacitor in the circuit. The capacitor charge that is lost in this way is replaced during the next cycle. The resultant charging current is integrated by the preamplifier circuit, which produces a voltage that is proportional to the radiant intensity. After amplification, the analog signal from the preamplifier passes into an analog-to-digital converter and to a microprocessor that controls the readout.

In using a diode-array transducer, the slit width of the spectrometer is usually adjusted so that the image of the entrance slit just fills the surface area of one of the diodes that make up the array. Thus the information obtained is equivalent to that recorded during scanning with a traditional spectrophotometer. With the array, however, information about the entire spectrum is accumulated essentially simultaneously and in discrete elements rather than in a continuous way.

Some of the photoconductor transducers mentioned in the previous section can also be fabricated into linear arrays for use in the infrared region.

Charge-Transfer Devices

Photodiode arrays cannot match the performance of photomultiplier tubes with respect to sensitivity, dynamic range, and signal-to-noise ratio. Thus, their use has been limited to experiments in which the multichannel advantage outweighs their shortcomings. In contrast, performance characteristics of charge-transfer devices appear to approach those of photomultiplier tubes in addition to having the multichannel advantage. As a consequence this type of transducer is now appearing in ever-increasing numbers in modern spectroscopic instruments.[24] A further advantage of charge-transfer devices is that they are two dimensional in the sense that individual transducer elements are arranged in rows and columns. For example, one detector that we describe in the next section consists of 244 rows of transducer ele-

[24] For details on charge-transfer devices, see J. V. Sweedler, *Crit. Rev. Anal. Chem.*, **1993**, *24*, 59; J. V. Sweedler, R. B. Bilhorn, P. M. Epperson, G. R. Sims, and M. B. Denton, *Anal. Chem.*, **1988**, *60*, 282A, 327A; *Charge-Transfer Devices in Spectroscopy*, J. V. Sweedler, K. L. Ratzlaff, and M. B. Denton, Eds. New York: Wiley, 1994.

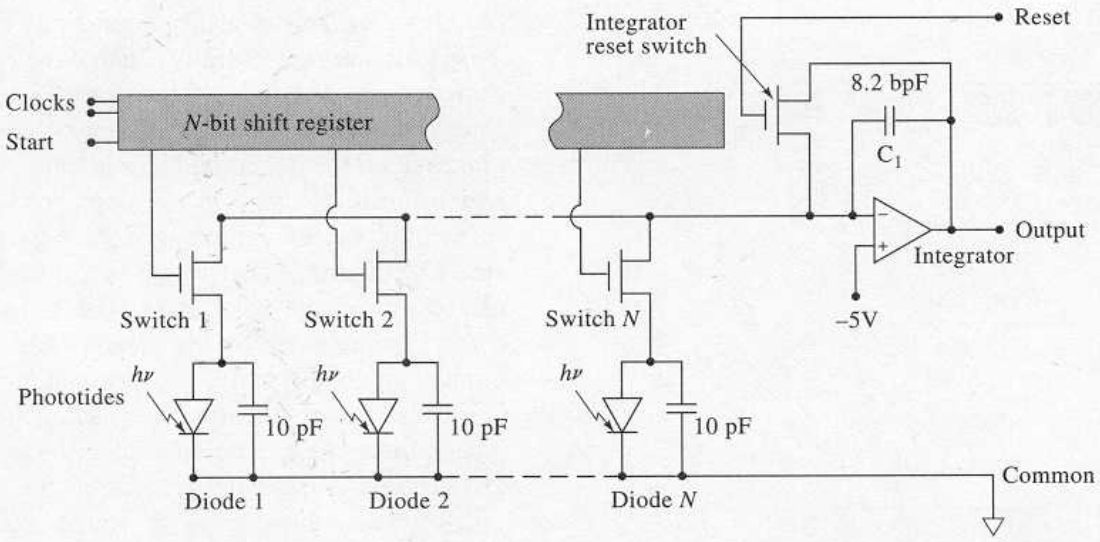

Figure 7-32 Block diagram of a photodiode-array detector chip.

ments, each row composed of 388 detector elements, resulting in a two-dimensional array of 19,672 individual transducers , or *pixels,* on a silicon chip with dimensions of 6.5 mm by 8.7 mm. With this device, it is possible to record an entire two-dimensional spectrum from an echelle spectrometer (Figure 7-21) simultaneously.

Charge-transfer devices operate much like a photographic film in that they integrate signal information as radiation strikes them. Figure 7-33 is a cross-sectional depiction of one of the pixels that composes a charge-transfer array. In this case, the pixel consists of two conductive electrodes that overlie an insulating layer of silica (note that a pixel in some charge-transfer devices is made up of more than two electrodes). This silica layer separates the electrodes from a region of *n*-doped silicon. This assemblage constitutes a metal oxide semiconductor capacitor that stores the charges formed when radiation strikes the doped silicon. When, as shown, a negative charge is applied to the electrodes, a charge inversion region is created under the electrodes, which is energetically favorable for the storage of holes. The mobile holes created by the absorption of photons then migrate and collect in this region. Typically, this region, which is called a *potential well,* is capable of holding as many as 10^5 to 10^6 charges before overflowing into an adjacent pixel. In the figure, one electrode is shown as more negative than the other, making the accumulation of charge under this electrode more favorable. The amount of charge generated during exposure to radiation is measured in either of two ways. In a *charge-injection device,* the voltage change that arises from movement of the charge from the region under one electrode to the region under the other is measured. In a *charge-coupled device,* the charge is moved to a charge-sensing amplifier for measurement.

Charge-Injection Devices. Figure 7-34 is a simplified diagram that shows the steps involved in the collection, storage, and measurement of the charge generated when one pixel of a semiconductor is exposed to photons. To monitor the intensity of the radiation that strikes the sensor element, the potentials applied to the capacitors are cycled as shown in steps (a) through (d) in the figure. In step (a), negative potentials are applied to the two electrodes, which leads to formation of potential wells that collect and store holes formed in the *n* layer by absorption of photons. Because the electrode on the right is at a more negative potential, all the holes are retained under this electrode initially. The magnitude of the charge collected in some brief time interval is deter-

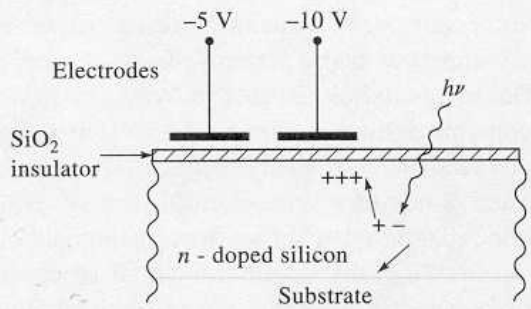

Figure 7-33 Cross section of a CTD detector in the charge integration mode. The positive hole produced by the photon *hν* is collected under the negative electrode.

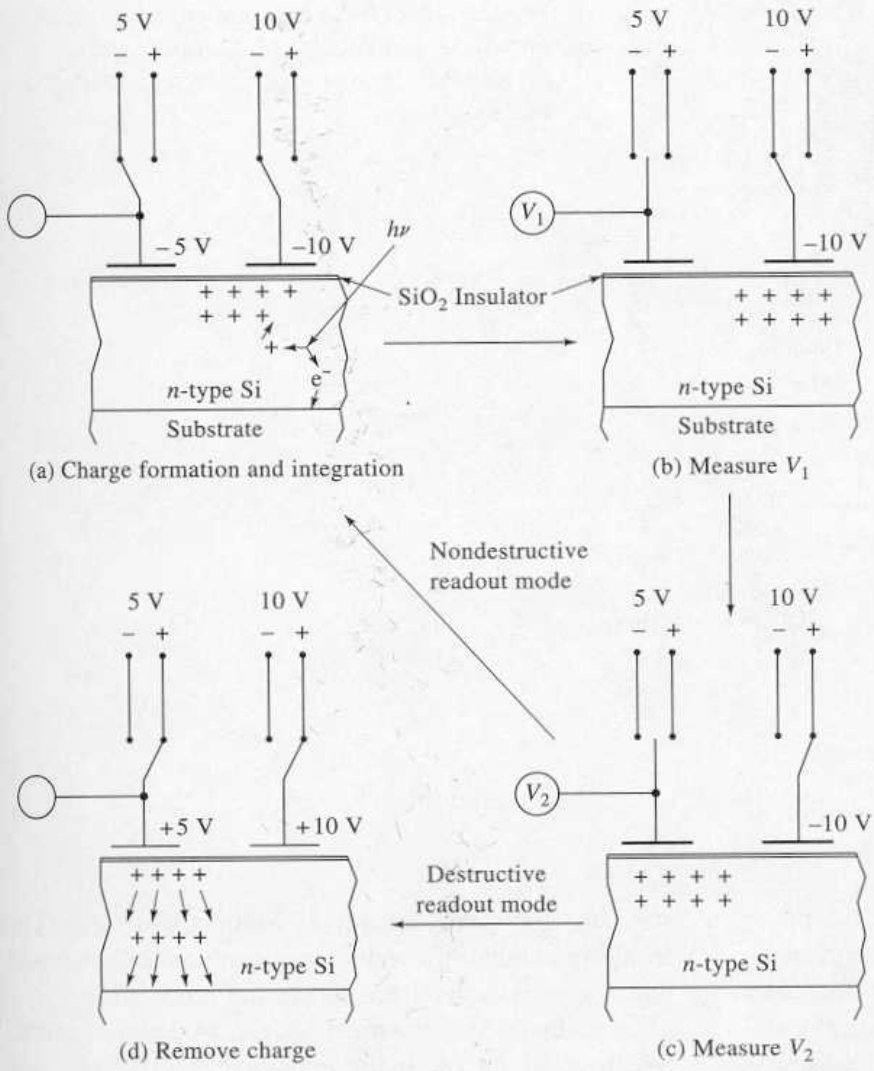

Figure 7-34 Duty cycle of a charge-injection device: (a) production and storage of charge, (b) first charge measurement, (c) second charge measurement after charge transfer, (d) reinjection of charge into the semiconductor.

mined in steps (b) and (c). In (b), the potential of the capacitor on the left (V_1) is determined after removal of its applied potential. In step (c), the holes that have accumulated on the right electrode are transferred to the potential well under the left electrode by switching the potential applied to the former from negative to positive. The new potential of the electrode V_2 is then measured. The magnitude of the accumulated charge is determined from the difference in potential ($V_1 - V_2$). In step (d), the detector is returned to its original state by applying positive potentials to both electrodes, which cause the holes to migrate toward the substrate. As an alternative to step (d), however, the detector can be returned to the condition shown in (a) without the loss of charge that has already accumulated. This process is called the *nondestructive readout mode* (NDRO). A major advantage of charge-injection devices over charge-coupled devices is that successive measurements can be made while integration is taking place.

As was true for the diode-array detector, the chip that contains the array of charge-injection transducer elements also contains appropriate integrated circuits for performing the cycling and measuring steps.

Charge-Coupled Device. Charge-coupled devices are marketed by several manufacturers and come in a variety of shapes and forms. Figure 7-35a illustrates the arrangement of individual detectors in a typical array that is made up of 512 × 320 pixels. Note that in this case the semiconductor is formed from *p*-type silicon, and the capacitor is biased positively so that electrons formed by the absorption of radiation collect in the well below the electrode, whereas holes move away from the *n*-type layer toward the substrate. Note also that each pixel is made up of three electrodes (labeled 1, 2, and 3 in Figure 7-35b) rather than two electrodes as in the charge-injection device. To measure the accumulated charge, a three-phase clock circuit is used to shift the

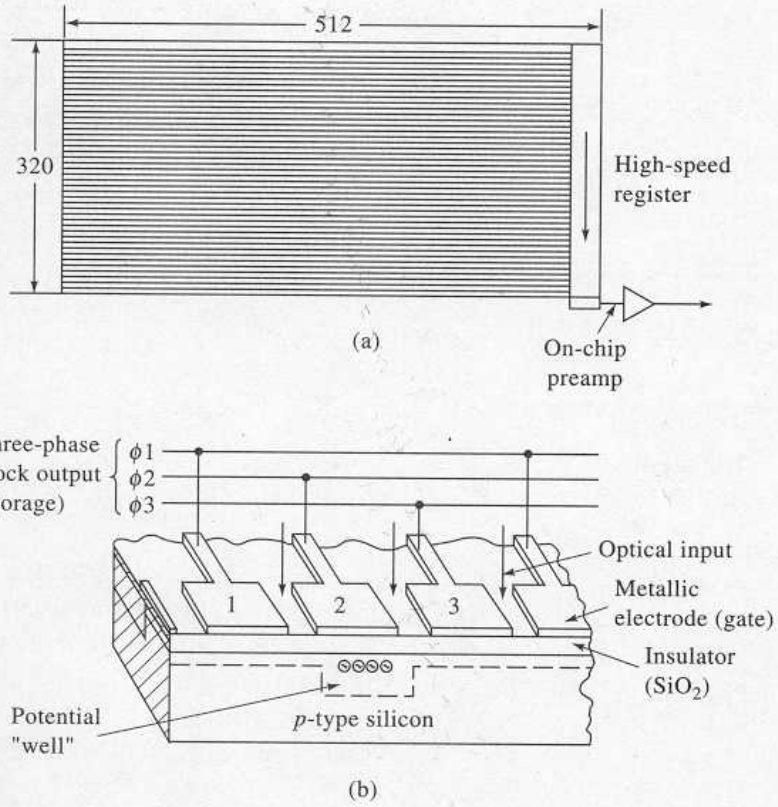

Figure 7-35 A charge-coupled device array: (a) arrangement of 512 × 320 pixels and (b) schematic showing four of the individual detectors.

charge in a stepwise manner to the right to the high-speed shift register shown in Figure 7-35a. The charges are then transferred downward to a preamplifier and then to the readout. Thus, a row-by-row scan of the detector surface is accomplished. In contrast to the charge injection device, the readout in this case neutralizes the accumulated charge. The charge-coupled device offers the advantage of greater sensitivity to low light levels. A disadvantage in some cases, however, is the destructive nature of the readout process.

7E-4 Photoconductivity Transducers

The most sensitive transducers for monitoring radiation in the near-infrared region (0.75 to 3 μm) are semiconductors whose resistances decrease when they absorb radiation within this range. The useful range of photoconductors can be extended into the far-infrared region by cooling to suppress noise that arises from thermally induced transitions among closely lying energy levels. This application of photoconductors is important in infrared Fourier transform instrumentation. Crystalline semiconductors are formed from the sulfides, selenides, and stibnides of such metals as lead, cadmium, gallium, and indium. Absorption of radiation by these materials promotes some of their bound electrons into an energy state in which they are free to conduct electricity. The resulting change in conductivity can then be measured with a circuit such as that shown in Figure 3-10a.

Lead sulfide is the most widely used photoconductive material that offers the advantage that it can be used at room temperature. Lead sulfide transducers are sensitive in the region between 0.8 and 3 μm (12,500 to 3300 cm^{-1}). A thin layer of this compound is deposited on glass or quartz plates to form the cell. The entire assembly is then sealed in an evacuated container to protect the semiconductor from reaction with the atmosphere. The sensitivity of cadmium sulfide, cadmium selenide, and lead sulfide transducers is shown by curves *B*, *D*, and *G* in Figure 7-25.

7E-5 Thermal Transducers[25]

The convenient phototransducers just considered are generally not applicable in the infrared because photons in this region lack the energy to cause photoemission of electrons. Thus, thermal transducers or transducers

[25] For a good discussion of optical radiation transducers of all types, including thermal detectors, see E. L. Dereniak and G. D. Growe, *Optical Radiation Detectors*. New York: Wiley, 1984.

based upon photoconduction (see Section 7E-4) must be employed. Neither of these is as satisfactory as photon transducers.

In thermal transducers, the radiation impinges upon and is absorbed by a small blackbody; the resultant temperature rise is measured. The radiant power level from a typical infrared beam is minute (10^{-7} to 10^{-9} W), so that the heat capacity of the absorbing element must be as small as possible if a detectable temperature change is to be produced. Every effort is made to minimize the size and thickness of the absorbing element and to concentrate the entire infrared beam on its surface. Under the best of circumstances, temperature changes are confined to a few thousandths of a kelvin.

The problem of measuring infrared radiation by thermal means is compounded by thermal noise from the surroundings. For this reason, thermal detectors are housed in a vacuum and are carefully shielded from thermal radiation emitted by other nearby objects. To further minimize the effects of extraneous heat sources, the beam from the source is generally chopped. In this way, the analyte signal, after transduction, has the frequency of the chopper and can be readily separated electronically from extraneous noise, which ordinarily varies only slowly with time.

Thermocouples

In its simplest form, a thermocouple consists of a pair of junctions formed when two pieces of a metal such as copper are fused to each end of a dissimilar metal such as constantan as shown in Figure 3-11. Between the two junctions a potential develops that varies with the *difference* in temperature of the junctions.

The transducer junction for infrared radiation is formed from very fine wires of bismuth and antimony or alternatively by evaporating the metals onto a nonconducting support. In either case, the junction is usually blackened to improve its heat-absorbing capacity and sealed in an evacuated chamber with a window that is transparent to infrared radiation.

The reference junction, which is usually housed in the same chamber as the active junction, is designed to have a relatively large heat capacity and is carefully shielded from the incident radiation. Because the analyte signal is chopped, only the difference in temperature between the two junctions is important; therefore, the reference junction does not need to be maintained at constant temperature. To enhance sensitivity, several thermocouples may be connected in series to fabricate what is called a *thermopile.*

A well-designed thermocouple transducer is capable of responding to temperature differences of 10^{-6} K. This difference corresponds to a potential difference of about 6 to 8 μV/μW. The thermocouple of an infrared detector is a low-impedance device that is usually connected to a high-impedance differential preamplifier, such as the field-effect transistor circuit shown in Figure 7-36. A voltage follower, such as that shown in Figure 3-7, is also used as a signal conditioner in thermocouple detector circuits.

Bolometers

A bolometer is a type of resistance thermometer constructed of strips of metals such as platinum or nickel, or from a semiconductor; the latter devices are often called *thermistors.* These materials exhibit a relatively large change in resistance as a function of temperature. The responsive element is kept small and blackened to absorb radiant heat. Bolometers are not so extensively used as other infrared transducers for the mid-infrared region. However, a germanium bolometer, operated at 1.5 K, is nearly an ideal transducer for radiation in the 5 to 400 cm^{-1} (2000 to 25 μm) range.

Pyroelectric Transducers

Pyroelectric transducers are constructed from single crystalline wafers of *pyroelectric materials,* which are insulators (dielectric materials) with very special thermal and electrical properties. Triglycine sulfate, $(NH_2CH_2COOH)_3 \cdot H_2SO_4$ (usually deuterated or with a fraction of the glycines replaced with alanine), is the most important pyroelectric material used in the construction of infrared transducers.

When an electric field is applied across any dielectric material, electric polarization takes place whose magnitude is a function of the dielectric constant of the material. For most dielectrics, this induced polarization rapidly decays to zero when the external field is removed. Pyroelectric substances, in contrast, retain a strong temperature-dependent polarization after removal of the field. Thus, by sandwiching the pyroelectric crystal between two electrodes (one of which is infrared transparent) a temperature-dependent capacitor is produced. Changing its temperature by irradiating it with infrared radiation alters the charge distribution across the crystal, which creates a measurable current in an external electric circuit that connects the two sides of the capacitor. The magnitude of this current is proportional to the surface area of the crystal and to its rate of change of polarization with temperature. Pyroelectric

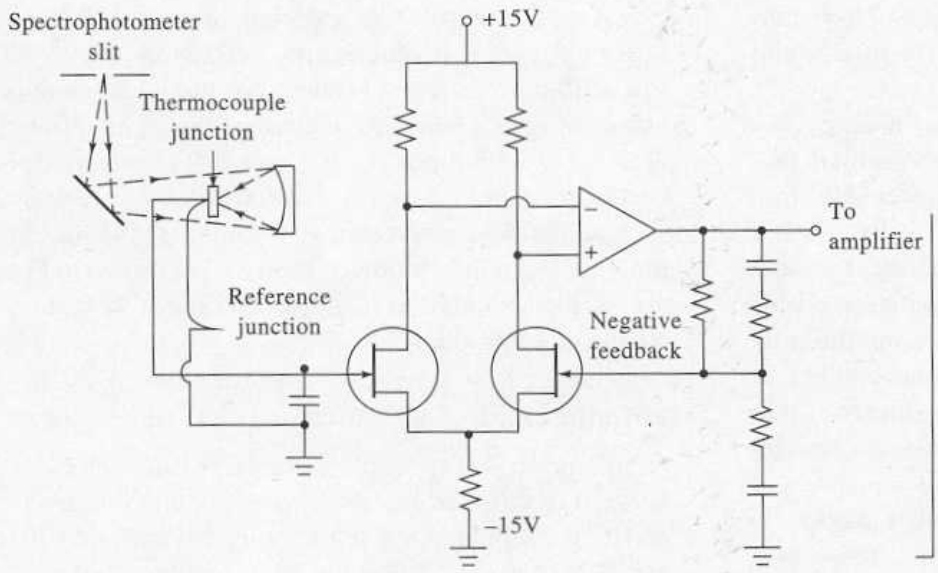

Figure 7-36 Thermocouple and preamplifier. *(Adapted from G. W. Ewing, J. Chem. Educ., **1971**, 48, A521. With permission.)*

crystals loose their residual polarization when they are heated to a temperature called the *Curie point.* For triglycine sulfate, the Curie point is 47°C.

Pyroelectric transducers exhibit response times that are fast enough to allow them to track the changes in the time-domain signal from an interferometer. For this reason, most Fourier transform infrared spectrometers employ this type of transducer.

7F SIGNAL PROCESSORS AND READOUTS

The signal processor is ordinarily an electronic device that amplifies the electrical signal from the transducer. In addition, it may alter the signal from dc to ac (or the reverse), change the phase of the signal, and filter it to remove unwanted components. Furthermore, the signal processor may be called upon to perform such mathematical operations on the signal as differentiation, integration, or conversion to a logarithm.

Several types of readout devices are found in modern instruments. Some of these devices include the d'Arsonval meter, digital meters, the scales of potentiometers, recorders, and cathode-ray tubes.

7F-1 Photon Counting

The output from a photomultiplier tube consists of a pulse of electrons for each photon that reaches the detector surface. Ordinarily this analog signal is filtered to remove undesirable fluctuations due to the random appearance of photons at the photocathode and measured as a dc voltage or current. If, however, the intensity of the radiation is too low to provide a satisfactory signal-to-noise ratio, it is possible, and often advantageous, to convert the analog signal to a train of digital pulses that may then be counted as discussed in Section 4C. Here, radiant power is proportional to the number of pulses per unit time rather than to an average current or potential. A measurement of this type is termed *photon counting.*

Counting techniques have been used for many years for measuring the power of X-ray beams and of radiation produced by the decay of radioactive species (these techniques are considered in detail in Chapters 12 and 32). Photon counting has also been applied to ultraviolet and visible radiation.[26] Here, the output of a photomultiplier tube is employed. In the previous section it was indicated that a single photon that strikes the cathode of a photomultiplier ultimately leads to a cascade of 10^6 to 10^7 electrons, which produces a pulse of current that can be amplified and counted.

Generally, the equipment for photon counting is similar to that shown in Figure 4-2 in which a comparator rejects pulses unless they exceed some predetermined minimum voltage. Comparators are useful for this task because dark current and instrument noise are

[26] For a review of photon counting, see H. J. Malmstadt, M. L. Franklin, and G. Horlick, *Anal. Chem.*, 1972, *44* (8), 63A.

often significantly smaller than the signal pulse and are thus not counted; an improved signal-to-noise ratio results.

Photon counting has a number of advantages over analog-signal processing, including improved signal-to-noise ratio, sensitivity to low radiation levels, improved precision for a given measurement time, and lowered sensitivity to photomultiplier tube voltage and temperature fluctuations. The required equipment is, however, more complex and expensive; the technique has thus not been widely applied for routine molecular absorption measurements in the ultraviolet and visible regions. It has, however, become the detection method of choice in fluorescence, chemiluminescence, and Raman spectrometry, where radiant power levels are low.

7G FIBER OPTICS

In the late 1960s, there began to appear on the market analytical instruments that contained fiber optics for transmitting radiation and images from one component of the instrument to another. These useful devices have added a new dimension to optical instrument designs.[27]

7G-1 Properties of Optical Fibers

Optical fibers are fine strands of glass or plastic that are capable of transmitting radiation for distances of several hundred feet or more. The diameter of optical fibers range from 0.05 μm to as large as 0.6 cm. Where images are to be transmitted, bundles of fibers, fused on the ends, are employed. A major application of these fiber bundles has been in medical diagnoses, where their flexibility permits transmission of images of organs through tortuous pathways to the physician. Filter optics are used not only for observation but also for illumination of objects; here, the ability to illuminate without heating is often of considerable importance.

Light transmission in an optical fiber takes place by total internal reflection as shown in Figure 7-37. In order for total internal reflections to occur, it is necessary that the transmitting fiber be coated with a material that has a refractive index that is somewhat smaller than the refractive index of the material from which the fiber is constructed. Thus, a typical glass fiber has a core with a refractive index of about 1.6 and has a glass sheath cladding with a refractive index of approximately 1.5. Typical plastic fibers have a polymethylmethacrylate core with a refractive index of 1.5 and have a polymer coating with a refractive index of 1.4.

A fiber, such as that shown in Figure 7-37, will transmit radiation contained in a limited incident cone with a half angle shown as θ in the figure. The *numerical aperture* of the fiber provides a measure of the magnitude of the so-called *acceptance cone.*

By suitable choice of construction materials, fibers that will transmit ultraviolet, visible, or infrared radiation can be manufactured. Several examples of their application to conventional analytical instruments will be found in the chapters that follow.

7G-2 Fiber-Optic Sensors

Fiber-optic sensors, which are also called *optrodes,* consist of a reagent phase immobilized on the end of a fiber optic.[28] Interaction of the analyte with the reagent creates a change in absorbance, reflectance, fluorescence, or luminescence, which is then transmitted to a detector via the optical fiber. Fiber-optic sensors are

[27] For a review of applications of fiber optics, see I. Chabay, *Anal. Chem.,* **1982**, *54,* 1071A and J. K. Crum, *Anal. Chem.,* **1969**, *41,* 26A.

[28] M. A. Arnold, *Anal. Chem.,* **1992**, *64,* 1015A; R. E. Dessy, *Anal. Chem.,* **1989**, *61,* 1079A; W. R. Seitz, *Anal. Chem.,* **1984**, *56,* 16A; S. Borman, *Anal. Chem.,* **1987**, *59,* 1161A; *Ibid.,* **1986**, *58,* 766A.

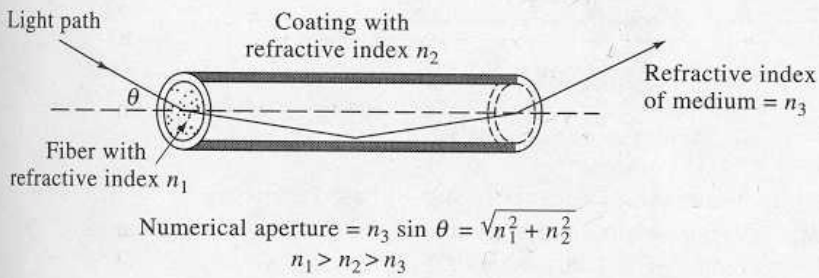

Figure 7-37 Schematic of the light path through an optical fiber.

generally simple, inexpensive devices that are easily miniaturized.

7G-3 Fiber Optics for Time Discrimination among Signals

An ingenious application of optical fibers is based on the use of strands of different lengths to vary the time of arrival at a single detector of optical signals from several sources. Time-resolved detection then permits the simultaneous determination of an analyte in several samples by means of a single detection system.[29] Figure 7-38a illustrates how such measurements are accomplished. At the heart of the detection system is a *star coupler*, a bidirectional device for coupling multiple

[29]R.L. Steffen and F.E. Lytle, *Anal. Chim. Acta*, ***1987***, *200*, 491.

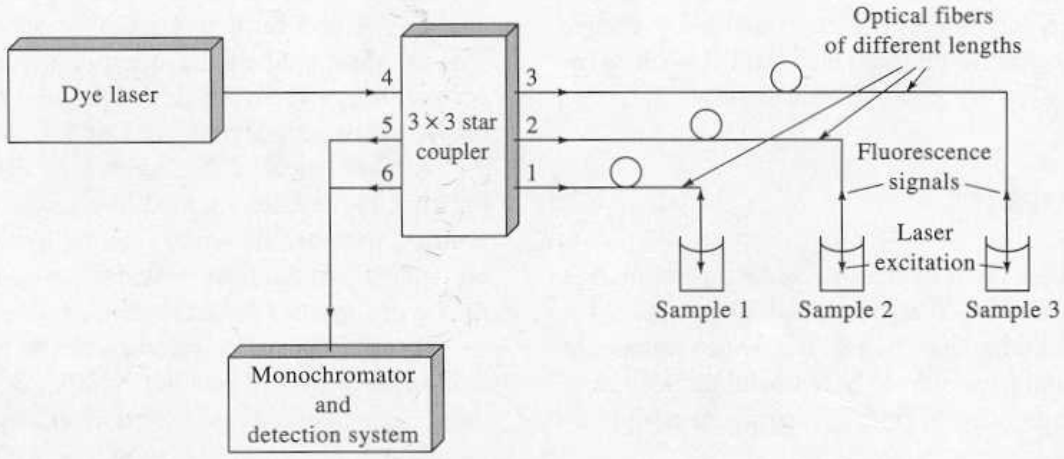

(a)

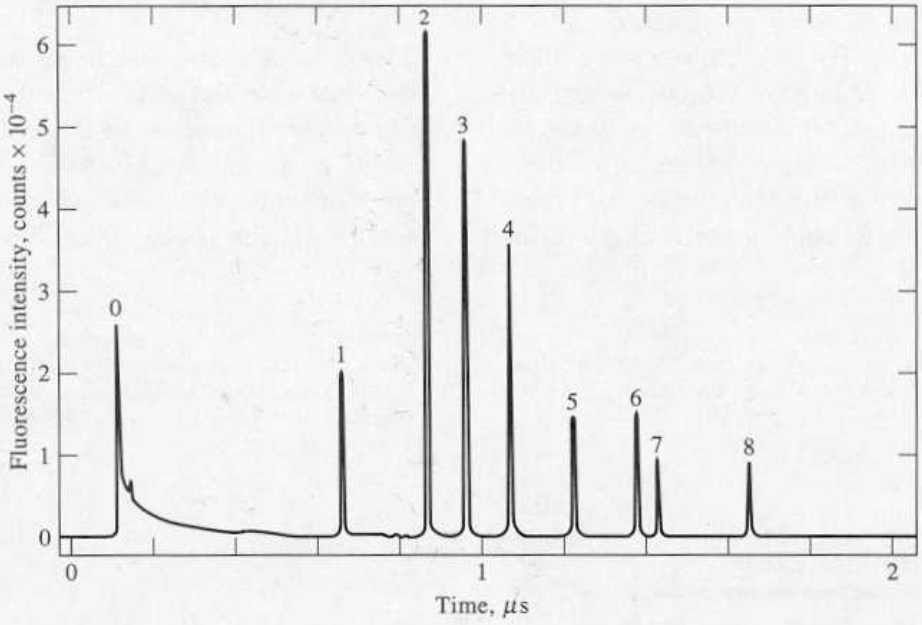

(b)

Figure 7-38 Instrument for exciting and separating fluorescence signals based upon the time of arrival of the signals at the transducer: (a) experimental arrangement; (b) output from the instrument. *(Reprinted with permission from R. L.Steffen and F. E. Lytle,* Anal. Chim. Acta, ***1987,*** 200, *491.)*

fiber optic bundles as illustrated in the figure. Star couplers are typically arranged in an $N \times N$ configuration, where N is the number of input ports and the number of output ports so that, as in this example of a 3×3 coupler, three fiber optic bundles may be conveniently coupled to three other bundles. Light entering any one of the six fibers is distributed approximately equally among all of the coupled fibers, including the input fiber. In other words, any light entering the star coupler via a fiber is distributed so that $1/(2N)$ of the incoming light emerges from each of the coupled fibers. In practice, the device is less than 100% efficient because some of the incoming light is lost at the coupling interfaces, but the emerging light is divided approximately equally among the six coupled fiber optic bundles in our example. It is important to recognize that although star couplers are mechanically configured as $N \times N$ devices, all $2N$ of the ports are identical optically and all of the ports are bidirectional.

In the time-correlated fluorescence experiment shown in Figure 7-38a, pulses of radiation from a dye laser pass into port 4 of the star coupler. The device divides the beam into six beams of approximately equal power, three of which are then directed into optical fibers 1, 2, and 3, which differ in length by several meters. About one sixth of the laser excitation passes back through fiber 4 unused. Approximately one third of the excitation emerges from ports 5 and 6 and passes to the detection system to serve as a time marker and power reference. The ends of fibers 1, 2, and 3 are inserted directly into three sample solutions where their output excites the analyte; this in turn produces pulses of fluorescence emission that travel in a reverse direction through the fibers as indicated by the arrowheads in Figure 7-38a. These pulses, however, return to the star coupler at different times. The radiation from sample 1 reaches the star coupler first via fiber 1 and is divided equally among all six of the ports. The fluorescence emission from ports 5 and 6 is then passed into a monochromator and thence to a nanosecond time-resolved detection system. At a subsequent time determined by the difference in the lengths of fiber 1 and fiber 2 and the velocity of light, the radiation from sample 2 arrives at the star coupler, and once again, the combined emission from fibers 5 and 6 is passed onto the detection system. This process is repeated for each of the sample fibers.

A plot of the output from the time-correlated single photon counting detection system is presented in Figure 7-38b for an experimental arrangement similar to that in Figure 7-38a. The system differs from that shown in the figure in that an 8×8 star coupler was used and 8 samples were analyzed. The data are presented as fluorescence intensity versus time of arrival of photons at the transducer. Note that there are nine peaks, the first of which (peak 0) corresponds to the laser excitation pulse mentioned previously. Peak 1 corresponds to a reference solution that was used in place of a sample in position 1 to correct the other peak intensities for fluctuations in the laser pulse power. Peaks 2 to 8 are fluorescence emission from the 7 samples. The magnitude of the peaks is proportional to the concentration of the analyte, 2-(1-naphthyl)-5-phenyloxazole, in the samples. Calibration curves for this detection scheme were linear over three orders of magnitude, and detection limits for the analyte were in the millimolar range and lower.

In the original experiments, optical fibers varying in length from 41 m to 142 m were used. Note that a laser pulse is delayed by roughly 50 ns or 0.05 μs for each 10 m of fiber that it traverses; modern electronic circuitry can easily discriminate among signals on this time scale. Several star coupler configurations were tested to determine the feasiblility of the detection scheme. In one case, a 4×4 coupler was used that permitted monitoring the fluorescence from four samples. By combining a 3×3 coupler with an 8×8 coupler, measurements were made on ten samples nearly simultaneously.

7H TYPES OF OPTICAL INSTRUMENTS

In this section, we define the terminology we will use to describe various types of optical instruments. It is important to realize that the nomenclature proposed here is not agreed upon and used by all scientists; it is simply a common nomenclature and the one that will be encountered throughout this book.

A *spectroscope* is an optical instrument used for the visual identification of atomic emission lines. It consists of a monochromator, such as one of those shown in Figure 7-16, in which the exit slit is replaced by an eyepiece that can be moved along the focal plane. The wavelength of an emission line can then be determined from the angle between the incident and dispersed beam when the line is centered on the eyepiece.

We use the term *colorimeter* to designate an instrument for absorption measurements in which the human eye serves as the detector using one or more color-comparison standards. A *photometer* consists of a source, a filter, and a photoelectric transducer as well as a signal processor and readout. It should be noted that some scientists and instrument manufacturers refer to photome-

ters as colorimeters or photoelectric colorimeters. Filter photometers are commercially available for absorption measurements in the ultraviolet, visible, and infrared regions, as well as emission and fluorescence in the first two wavelength regions. Photometers designed for fluorescence measurements are also called *fluorometers.*

A *spectrograph* is similar in construction to the two monochromators shown in Figure 7-16 except that the slit arrangement is replaced with a large aperture that holds a detector or transducer that is continuously exposed to the entire spectrum of dispersed radiation. Historically, the detector was a photographic film or plate. Currently, however, diode arrays or charge-transfer devices are often used as transducers in spectrographs.

A *spectrometer* is an instrument that provides information about the intensity of radiation as a function of wavelength or frequency. The dispersing modules in some spectrometers are multichannel so that two or more frequencies can be viewed simultaneously. Such instruments are sometimes called *polychromators.* A *spectrophotometer* is a spectrometer equipped with one or more exit slits and photoelectric transducers that permit the determination of the ratio of the power of two beams as a function of wavelength as in absorption spectroscopy. A spectrophotometer for fluorescence analysis is sometimes called a *spectrofluorometer.*

All of the instruments named in this section thus far employ filters or monochromators to isolate a portion of the spectrum for measurement. A *multiplex* instrument, in contrast, obtains spectral information without first dispersing or filtering the radiation to provide wavelengths of interest. The term *multiplex* comes from communication theory, where it is used to describe systems in which many sets of information are transported simultaneously through a single channel. Multiplex analytical instruments then are single-channel devices in which all components of an analytical response are collected *simultaneously.* In order to determine the magnitude of each of these components, it is necessary to modulate the analyte signal in a way that permits subsequent decoding of the response into its components.

Most multiplex analytical instruments depend upon the *Fourier transform* (FT) for signal decoding and are consequently often called Fourier transform spectrometers. Such instruments are by no means confined to optical spectroscopy. Indeed, Fourier transform devices have been described for nuclear magnetic resonance spectrometry, mass, and microwave spectroscopy. Several of these instruments will be described in some detail in subsequent chapters. The section that follows describes the principles on which Fourier transform optical spectrometers are based.

7I PRINCIPLES OF FOURIER TRANSFORM OPTICAL MEASUREMENTS

Fourier transform spectroscopy was first developed by astronomers in the early 1950s in order to study the infrared spectra of distant stars; only by the Fourier technique could the very weak signals from these sources be isolated from environmental noise. The first chemical applications of Fourier transform spectroscopy, which were reported approximately a decade later, were to the energy-starved far-infrared region; by the late 1960s, instruments for chemical studies in both the far-infrared (10 to 400 cm^{-1}) and the ordinary infrared regions were available commercially. Descriptions of Fourier transform instruments for the ultraviolet and visible spectral regions can also be found in the literature, but their adoption has been less widespread.[30]

7I-1 Inherent Advantages of Transform Spectrometry

There are several major advantages to the use of Fourier transform instruments. The first is the *throughput,* or *Jaquinot, advantage,* which is realized because Fourier transform instruments have few optical elements and no slits to attenuate radiation. As a consequence, the power of the radiation that reaches the detector is much greater than that in dispersive instruments, and much greater signal-to-noise ratios are observed.

A second advantage of Fourier transform instruments is their extremely high resolving power and wavelength reproducibility that make possible the analysis of complex spectra in which the sheer number of lines and spectral overlap make the determination of

[30] For more complete discussions of optical Fourier transform spectroscopy, consult the following references: A. G. Marshall and F. R. Verdun, *Fourier Transforms in NMR, Optical, and Mass Spectrometry.* New York: Elsevier, 1990; A. G. Marshall, *Fourier, Hadamard, and Hilbert Transforms in Chemistry.* New York: Plenum Press, 1982; *Transform Techniques in Chemistry,* P. R. Griffiths, Ed. New York: Plenum Press, 1978. For brief reviews, see P. R. Griffiths, *Science,* **1983**, *222*, 297; W. D. Perkins, *J. Chem. Educ.,* **1986**, *63*, A5, A296; L. Glasser, *J. Chem. Educ.,* **1987**, *64*, A228, A260, A306.

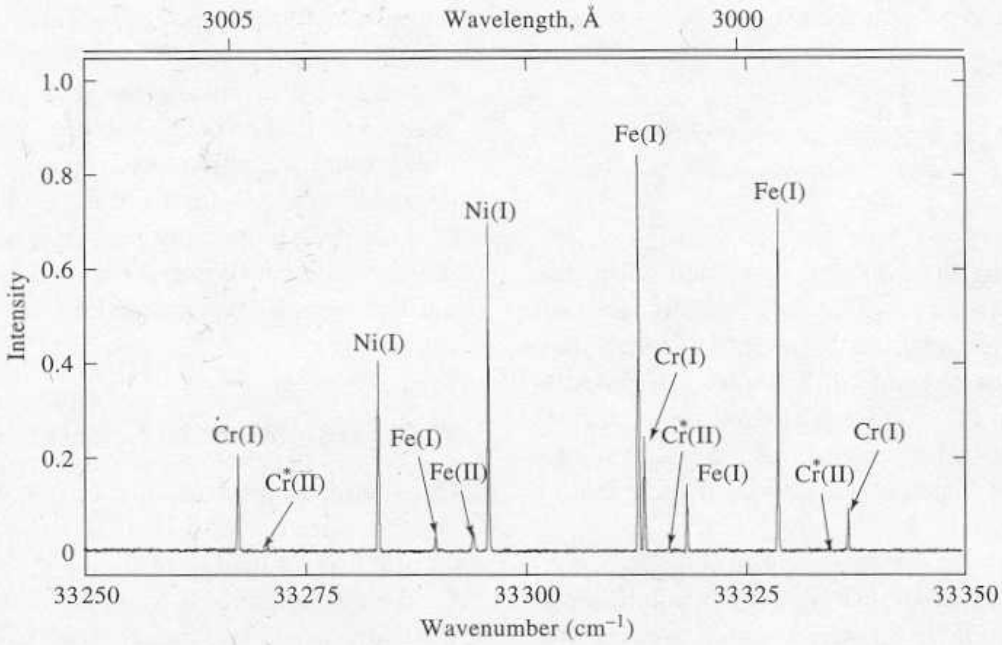

Figure 7-39 An iron emission spectrum illustrating the high resolving power of a Fourier transform emission spectrometer. *(Reprinted with permission from A. P. Thorne,* Anal. Chem., ***199,*** *63, 63A. Copyright 1991 American Chemical Society.)*

individual spectral features difficult. Figure 7-39, which is part of an emission spectrum for a steel, illustrates this advantage. The spectrum, which in Figure 7-39 extends from only 299.85 to 300.75 nm, contains 13 well-separated lines of three elements. The wavelength resolution ($\Delta\lambda/\lambda$) for the closest pair of lines is about 6 ppm.

A third advantage arises because all elements of the source reach the detector simultaneously. This characteristic makes it possible to obtain data for an entire spectrum in one second or less. Let us examine the consequences of this last advantage in further detail.

For purposes of this discussion, it is convenient to think of an experimentally derived spectrum as made up of m individual transmittance measurements at equally spaced frequency or wavelength intervals called *resolution elements.* The quality of the spectrum—that is, the amount of spectral detail—increases as the number of resolution elements becomes larger or as the frequency intervals between measurements become smaller.[31] Thus, in order to increase spectral quality, m must be made larger; clearly, increasing the number of resolution elements must also increase the time required for obtaining a spectrum with a scanning instrument.

Consider, for example, the derivation of an infrared spectrum from 500 to 5000 cm^{-1}. If resolution elements of 3 cm^{-1} were chosen, m would be 1500; if 0.5 s were required for recording the transmittance of each resolution element, 750 s or 12.5 min would be needed to obtain the spectrum. Reducing the width of the resolution element to 1.5 cm^{-1} would be expected to provide significantly greater spectral detail; it would also double the number of resolution elements as well as the time required for their measurement.

For most optical instruments, particularly those designed for the infrared region, decreasing the width of the resolution element has the unfortunate effect of decreasing the signal-to-noise ratio because narrower slits must be used, which lead to weaker source signals that reach the transducer. For infrared detectors, the reduction in signal strength is not, however, accompanied by a corresponding decrease in detector noise. Therefore, a degradation in signal-to-noise ratio results.

On page 108, it was pointed out that marked improvements in signal-to-noise ratios accompany signal averaging. Here, it was shown (Equation 5-11) that the

[31] With a recording spectrophotometer, of course, individual point-by-point measurements are not made; nevertheless, the idea of a resolution element is useful, and the ideas generated from it apply to recording instruments as well.

signal-to-noise ratio *S/N* for the average of n measurements is given by

$$\frac{S}{N} = \sqrt{n}\,\frac{S_x}{\sqrt{\sum_{i=1}^{n}(S_x - S_i)^2}} = \frac{S_x}{N_x}\sqrt{n} \quad (7\text{-}20)$$

where S_x and N_x are the averaged signal and noise. The application of signal averaging to conventional spectroscopy is, unfortunately, costly in terms of time. Thus, in the example just considered, 750 s were required to obtain a spectrum of 1500 resolution elements. To improve the signal-to-noise ratio by a factor of 2 would require averaging 4 spectra, which would then require 4×750 s or 50 min.

Fourier transform spectroscopy differs from conventional spectroscopy in that all of the resolution elements for a spectrum are measured *simultaneously,* thus reducing enormously the time required to obtain a spectrum at any chosen signal-to-noise ratio. An entire spectrum of 1500 resolution elements can then be recorded in about the time required to observe just one element by conventional spectroscopy (0.5 s in our earlier example). This large decrease in observation time is often used to markedly enhance the signal-to-noise ratio of Fourier transform measurements. For example, in the 750 s required to derive the spectrum by scanning, 1500 Fourier transform spectra could be recorded and averaged. According to Equation 7-20, the improvement in signal-to-noise ratio would be $\sqrt{1500}$ or about 39. This inherent advantage of Fourier transform spectroscopy was first recognized by P. Fellgett in 1958 and is termed the *Fellgett,* or *multiplex, advantage.* It is worth noting here that for several reasons, the theoretical $\sqrt{n}$ improvement in *S/N* is seldom entirely realized. Nonetheless, major gains in signal-to-noise ratios are generally observed with the Fourier transform technique.

The multiplex advantage is important enough so that nearly all infrared spectrometers are of the Fourier transform type. Fourier transform instruments are much less common for the ultraviolet, visible, and near-infrared regions, however, because signal-to-noise limitations for spectral measurements with these types of radiation seldom lies in detector noise but instead in shot noise and flicker noise associated with the source. In contrast to detector noise, the magnitudes of both shot and flicker noise increase as the power of the signal increases. Furthermore, the total noise for all of the resolution elements in a Fourier transform measurement tends to be averaged and spread out uniformly over the entire transformed spectrum. Thus, the signal-to-noise ratio for strong peaks in the presence of weak peaks is improved by averaging but degraded for the weaker peaks. For flicker noise, such as is encountered in the background radiation from many spectral sources, degradation of *S/N* for all peaks is observed. This effect is sometimes termed the *multiplex disadvantage* and is largely responsible for the fact the Fourier transform has not been widely applied for ultraviolet/visible spectroscopy.[32]

7I-2 Time-Domain Spectroscopy

Conventional spectroscopy can be termed *frequency-domain* spectroscopy in that radiant power data are recorded as a function of frequency or the inversely related wavelength. In contrast, *time-domain* spectroscopy, which can be achieved by the Fourier transform, is concerned with changes in radiant power with *time.* Figure 7-40 illustrates the difference.

The plots in Figures 7-40c and 7-40d are conventional spectra of two monochromatic sources with frequencies ν_1 and ν_2 Hz. The curve in Figure 7-40e is the spectrum of a source that contains both frequencies. In each case, some measure of the radiant power, $P(\nu)$ is plotted with respect to the frequency in hertz. The symbol in parentheses is added to emphasize the frequency dependence of the power; time-domain power will be indicated by $P(t)$.

The curves in Figure 7-40a show the time-domain spectra for each of the monochromatic sources. The two have been plotted together in order to make the small frequency difference between them more obvious. Here, the instantaneous power $P(t)$ is plotted as a function of time. The curve in Figure 7-40b is the time-domain spectrum of the source that contains the two frequencies. As is shown by the horizontal arrow, the plot exhibits a periodicity or *beat* as the two waves go in and out of phase.

Examination of Figure 7-41 reveals that the time-domain signal from a source that contains several wavelengths is considerably more complex than those shown in Figure 7-40. Because a large number of wavelengths are involved, a full cycle is not completed in the time period shown. To be sure, a pattern of beats can be ob-

[32] For a further description of this *multiplex disadvantage* in atomic spectroscopy, see A. P. Thorne, *Anal. Chem.,* **1991**, *63,* 62A-63A; A. G. Marshall and F. R. Verdun, *Fourier Transforms in NMR, Optical, and Mass Spectrometry,* Chapter 5. New York: Elsevier, 1990.

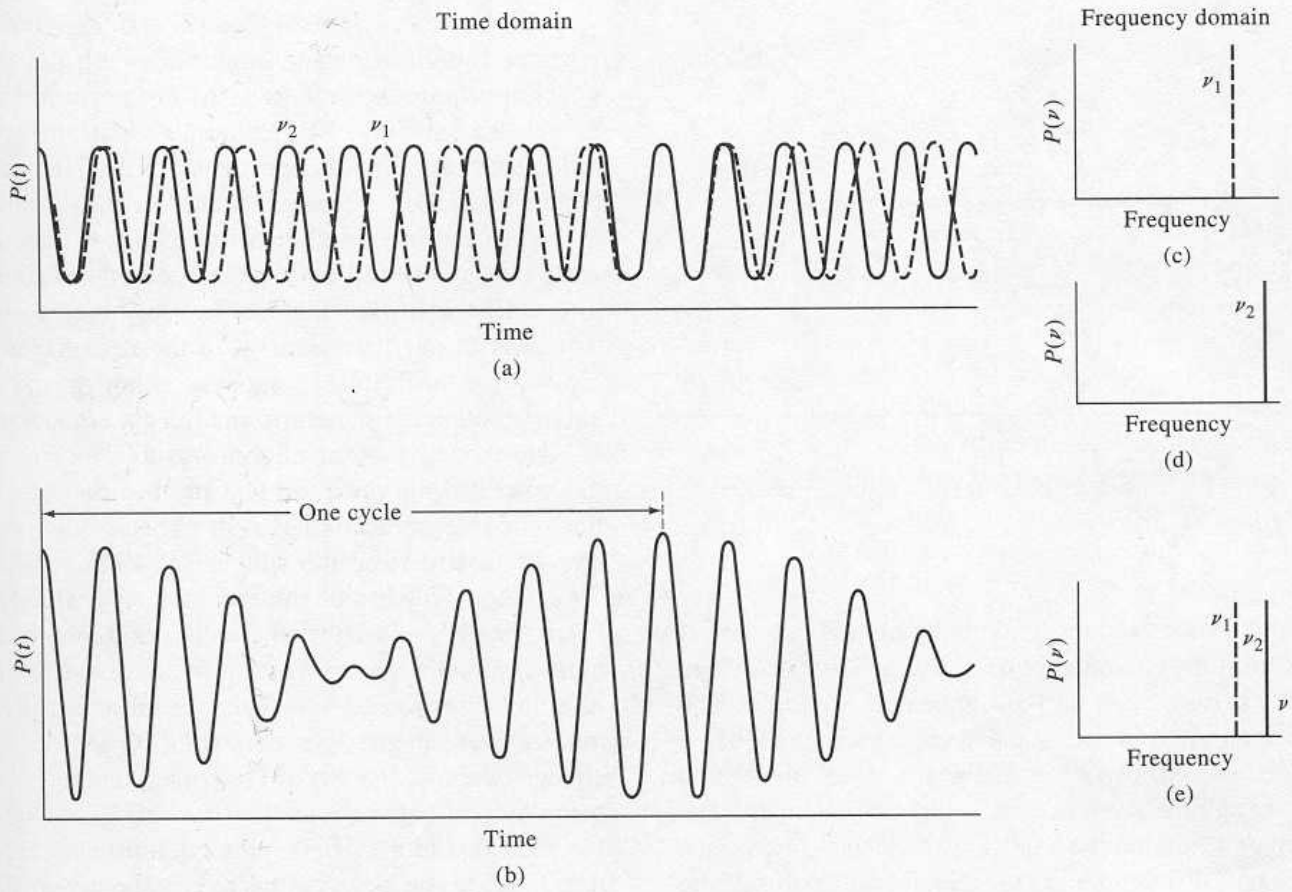

Figure 7-40 Illustrations of (1) time-domain plots (a) and (b) and (2) frequency-domain plots (c), (d), and (e).

served as certain wavelengths pass in and out of phase. In general, the signal power decreases with time as a consequence of the various closely spaced wavelengths becoming more and more out of phase.

It is important to appreciate that a time-domain signal contains the same information as a spectrum does in the frequency domain, and in fact, one can be converted to the other by numerical computations. Thus, Figure 7-40b was derived from Figure 7-40e by means of the equation

$$P(t) = k \cos (2\pi\nu_1 t) + k \cos (2\pi\nu_2 t) \quad (7\text{-}21)$$

where k is a constant and t is the time. The difference in frequency between the two lines was approximately 10% of ν_2.

The interconversion of time- and frequency-domain signals is exceedingly complex and mathematically tedious when more than a few lines are involved; the operation is only practical with a high-speed computer.

7I-3 Obtaining Time-Domain Spectra with a Michelson Interferometer

Time-domain signals, such as those shown in Figures 7-40 and 7-41, cannot be acquired experimentally with radiation of the frequency range that is associated with optical spectroscopy (10^{12} to 10^{15} Hz) because there are no transducers that will respond to power variations at these enormous frequencies. Thus, a typical transducer yields a signal that corresponds to the average power of a high-frequency signal and not to its periodic variation. To obtain time-domain signals requires, therefore, a method of converting (or *modulating*) a high-frequency signal to one of measurable frequency without distorting the time relationships carried in the signal; that is, the frequencies in the modulated signal must be directly proportional to those in the original. Different signal-modulation procedures are employed for the various wavelength regions of the spectrum. The *Michelson interferometer* is used extensively to modulate radiation in the optical region.

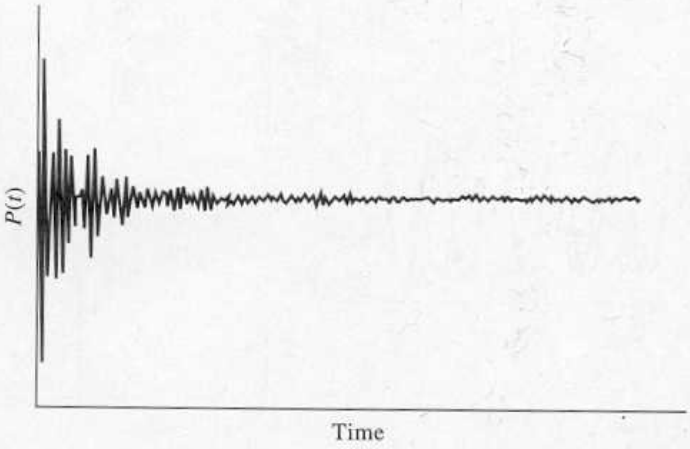

Figure 7-41 Time-domain signal of a source made up of several wavelengths.

The device used for modulating optical radiation is an interferometer similar in design to one first described by Michelson late in the nineteenth century. The Michelson interferometer is a device that splits a beam of radiation into two beams of nearly equal power and then recombines them in such a way that intensity variations of the combined beam can be measured as a function of differences in the lengths of the paths of the two beams. Figure 7-42 is a schematic of such an interferometer as it is used for optical Fourier transform spectroscopy.

As shown in Figure 7-42, a beam of radiation from a source is collimated and impinges on a beam splitter, which transmits approximately half of the radiation and reflects the other half. The resulting twin beams are then reflected from mirrors, one of which is fixed and the other of which is movable. The beams then meet again at the beam splitter, with half of each beam directed toward the sample and detector and the other two halves directed back toward the source. Only the two halves that pass through the sample to the detector are employed for analytical purposes, although the other halves contain the same information about the source.

Horizontal motion of the movable mirror causes the power of the radiation that reaches the detector to fluctuate in a predictable manner. When the two mirrors are equidistant from the splitter (position 0 in Figure 7-42), the two parts of the recombined beam are precisely in phase and the power is a maximum. For a monochromatic source, motion of the movable mirror in either direction by a distance equal to exactly one-quarter wavelength (position B or C in the figure) changes the path length of the corresponding reflected beam by one-half wavelength (one-quarter wavelength for each direction). Under this circumstance, destructive interference reduces the radiant power of the recombined beams to zero. Further motion to A and D brings the two halves back in phase so that constructive interference again occurs.

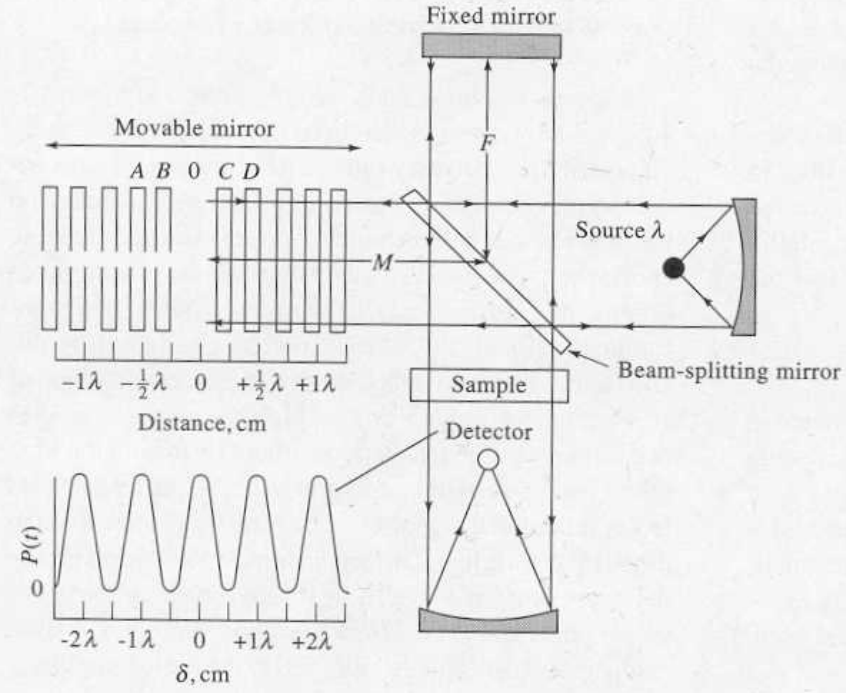

Figure 7-42 Schematic of a Michelson interferometer illuminated by a monochromatic source.

The difference in path lengths for the two beams, $2(M - F)$ in the figure is termed the *retardation* δ. A plot of the output power from the detector versus δ is called an *interferogram;* for monochromatic radiation, the interferogram takes the form of a cosine curve such as that shown in the lower left of Figure 7-42 (cosine rather than sine because the power is always a maximum when δ is zero and the two paths are identical).

The radiation striking the detector after passing through a Michelson interferometer will generally be much lower in frequency than the source frequency. The relationship between the two frequencies is derived by reference to $P(t)$ versus δ plot in Figure 7-42. One cycle of the signal occurs when the mirror moves a distance that corresponds to one half a wavelength ($\lambda/2$). If the mirror is moving at a constant velocity of v_M, and we define τ as time required for the mirror to move $\lambda/2$ cm, we may write

$$v_M \tau = \frac{\lambda}{2} \tag{7-22}$$

The frequency f of the signal at the detector is simply the reciprocal of τ, or

$$f = \frac{1}{\tau} = \frac{v_M}{\lambda/2} = \frac{2v_M}{\lambda} \tag{7-23}$$

We may also relate this frequency to the wavenumber $\bar{\nu}$ of the radiation. Thus,

$$f = 2v_M\bar{\nu} \tag{7-24}$$

The relationship between the *optical frequency* of the radiation and the frequency of the interferogram is obtained by substitution of $\lambda = c/\nu$ into Equation 7-23. Thus,

$$f = \frac{2v_M}{c}\nu \tag{7-25}$$

where ν is the frequency of the radiation and c is the velocity of light (3×10^{10} cm/s). When] v_M is constant, it is evident that the *interferogram frequency f is directly proportional to the optical frequency* ν. Furthermore, the proportionality constant will generally be a very small number. For example, if the mirror is driven at a rate of 1.5 cm/s,

$$\frac{2v_M}{c} = \frac{2 \times 1.5 \text{ cm/s}}{3 \times 10^{10} \text{ cm/s}} = 10^{-10}$$

and

$$f = 10^{-10}\,\nu$$

As shown by the following example, the frequency of visible and infrared radiation is readily modulated into the audio range by a Michelson interferometer.

EXAMPLE 7-3

Calculate the frequency range of a modulated signal from a Michelson interferometer with a mirror velocity of 0.20 cm/s, for visible radiation of 700 nm and infrared radiation of 16 μm (4.3×10^{14} to 1.9×10^{13} Hz).

Employing Equation 7-23, we find

$$f_1 = \frac{2 \times 0.20 \text{ cm/s}}{700 \text{ nm} \times 10^{-7} \text{ cm/nm}} = 5700 \text{ Hz}$$

$$f_2 = \frac{2 \times 0.20 \text{ cm/s}}{16 \ \mu\text{m} \times 10^{-4} \text{ cm/}\mu\text{m}} = 250 \text{ Hz}$$

Certain types of visible and infrared transducers are capable of following fluctuations in signal power that fall into the audio-frequency range. Thus, it becomes possible to record a modulated time-domain signal that reflects exactly the appearance of the very high-frequency time-domain signal from a visible or infrared source. Figure 7-43 shows three examples of such time-domain interferograms on the left and their frequency-domain spectra on the right.

Fourier Transformation of Interferograms

The cosine wave of the interferogram shown in Figure 7-43a (and also in Figure 7-42) can be described in theory by the equation

$$P(\delta) = \frac{1}{2} P(\bar{\nu}) \cos 2\pi f t \tag{7-26}$$

where $P(\bar{\nu})$ is the radiant power of the beam that is incident upon the interferometer and $P(\delta)$ is the amplitude or power of the interferogram signal. The parenthetical symbols emphasize that one power is in the frequency domain and the other is in the time domain. In practice, the foregoing equation is modified to take into account the fact that the interferometer ordinarily will not split the source exactly in half and that the detector response and the amplifier behavior are frequency dependent. Thus, it is useful to introduce a new variable $B(\bar{\nu})$ which depends upon $P(\bar{\nu})$ but also takes these factors

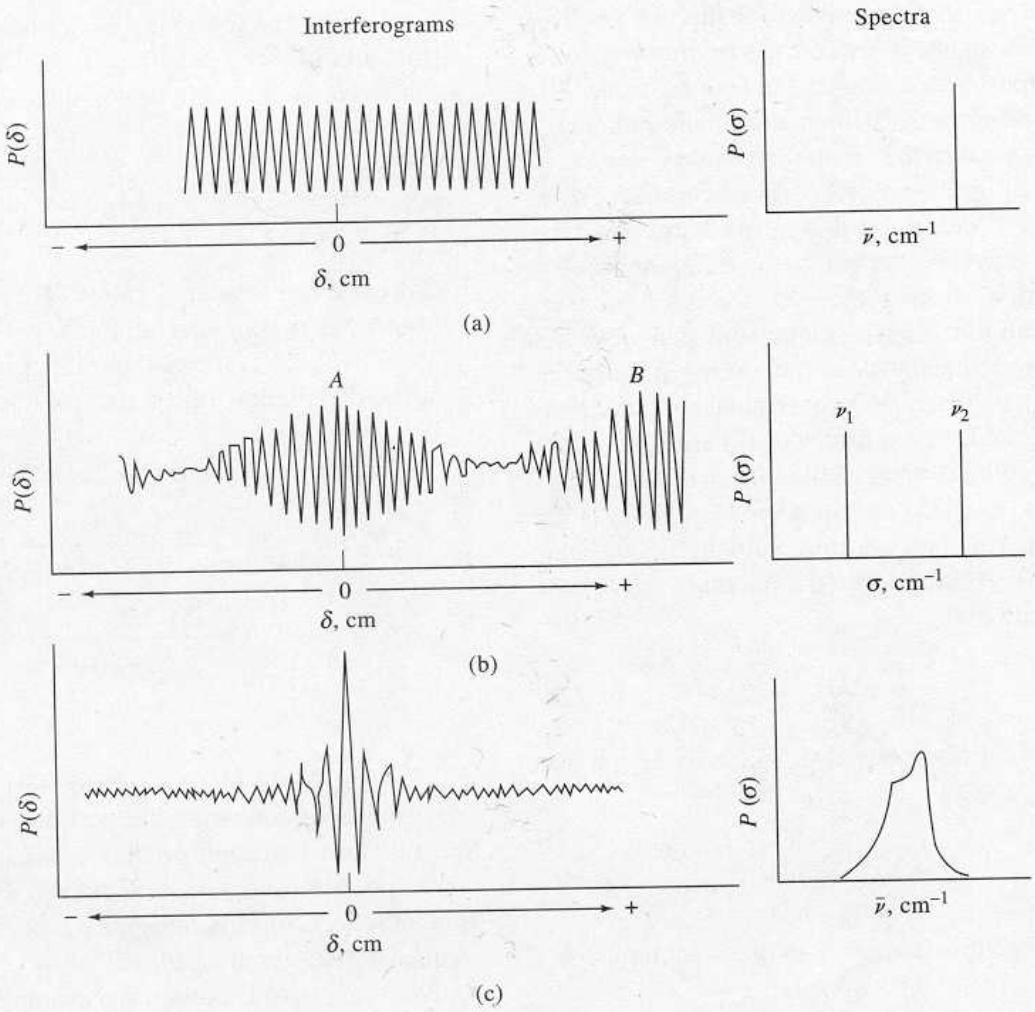

Figure 7-43 Comparison of interferograms and optical spectra.

into account. Therefore, we rewrite the equation in the form

$$P(\delta) = B(\bar{\nu}) \cos 2\pi ft \tag{7-27}$$

Substitution of Equation 7-24 into Equation 7-26 leads to

$$P(\delta) = B(\bar{\nu}) \cos 4\pi v_M \bar{\nu} t \tag{7-28}$$

But the mirror velocity can be expressed in terms of retardation or

$$v_M = \frac{\delta}{2t}$$

Substitution of this relationship into Equation 7-28 gives

$$P(\delta) = B(\bar{\nu}) \cos 2\pi\delta\bar{\nu}$$

which expresses the magnitude of the interferogram signal as a function of the retardation factor and the wavenumber of the optical input signal.

The interferograms shown in Figure 7-43b can be described by two terms, one for each wavenumber. Thus,

$$P(\delta) = B_1(\bar{\nu}) \cos 2\pi\delta\bar{\nu}_1 + B_2(\bar{\nu}) \cos 2\pi\delta\bar{\nu}_2 \tag{7-29}$$

For a continuum source, as in Figure 7-43c, the interferogram can be represented as a sum of an infinite number of cosine terms. That is,

$$P(\delta) = \int_{-\infty}^{+\infty} B(\bar{\nu}) \cos 2\pi\bar{\nu}\delta d\bar{\nu} \tag{7-30}$$

The Fourier transform of this integral is

$$B(\bar{\nu}) = \int_{-\infty}^{+\infty} P(\delta) \cos 2\pi\bar{\nu}\delta d\delta \tag{7-31}$$

A complete Fourier transformation requires both real (cosine) and imaginary (sine) components; we have presented only the cosine part, which is sufficient for manipulating real/even functions.

Optical Fourier transform spectroscopy consists of recording $P(\delta)$ as a function of δ (Equation 7-30) and then mathematically transforming this relation to one that gives $B(\bar{\nu})$ as a function of $\bar{\nu}$ (the frequency spectrum) as shown by Equation 7-31.

Equations 7-30 and 7-31 cannot be employed as written because they assume that the beam contains radiation from zero to infinite wavenumbers and a mirror drive of infinite length. Furthermore, Fourier transformations with a computer require that the detector output be digitized; that is, the output must be sampled periodically and stored in digital form. Equation 7-31 however, demands that the sampling intervals $d\delta$ be infinitely small; that is, $d\delta \rightarrow 0$. From a practical standpoint, only a finite-sized sampling interval can be summed over a finite retardation range of a few centimeters. These constraints have the effect of limiting the resolution of a Fourier transform instrument and restricting its frequency range.

Resolution

The resolution of a Fourier transform spectrometer can be described in terms of the difference in wavenumber between two lines that can be just separated by the instrument. That is,

$$\Delta\bar{\nu} = \bar{\nu}_1 - \bar{\nu}_2 \qquad (7\text{-}32)$$

where $\bar{\nu}_1$ and $\bar{\nu}_2$ are wavenumbers for a pair of barely resolvable lines.

It is possible to show that in order to resolve two lines, the time-domain signal must be scanned long enough so that one complete cycle or beat for the two lines is completed; only then will all of the information contained in the spectrum have been recorded. For example, resolution of the two lines $\bar{\nu}_1$ and $\bar{\nu}_2$ in Figure 7-43b requires recording the interferogram from the maximum A at zero retardation to the maximum B where the two waves are again in phase. The maximum at B occurs, however, when $\delta\bar{\nu}_2$ is larger than $\delta\bar{\nu}_1$ by 1 in Equation 7-29. That is, when

$$\delta\bar{\nu}_2 - \delta\bar{\nu}_1 = 1$$

or

$$\bar{\nu}_2 - \bar{\nu}_1 = \frac{1}{\delta}$$

Substitution into Equation 7-32 reveals that the resolution is given by

$$\Delta\bar{\nu} = \bar{\nu}_2 - \bar{\nu}_1 = \frac{1}{\delta} \qquad (7\text{-}33)$$

This equation means that resolution in wavenumbers will improve in proportion to the reciprocal of the distance that the mirror travels.

EXAMPLE 7-4

What length of mirror drive will provide a resolution of 0.1 cm^{-1}? Substituting into Equation 7-33 gives

$$0.1 = \frac{1}{\delta}$$

$$\delta = 10 \text{ cm}$$

The mirror motion required is one half the retardation, or 5 cm.

Instruments

Details about modern Fourier transform optical spectrometers are found in Section 16C-1. An integral part of these instruments is a sophisticated computer for controlling data acquisition, for storing data, for signal averaging, and for performing the Fourier transformations.

7J QUESTIONS AND PROBLEMS

7-1 Why must the slit width of a prism monochromator be varied to provide constant effective bandwidths whereas a nearly constant slit width may be used with a grating monochromator?

7-2 Why do quantitative and qualitative analyses often require different monochromator slit widths?

7-3 The Wien displacement law states that the wavelength maximum in micrometers for blackbody radiation is given by the relationship

$$\lambda_{max} T = 2.90 \times 10^3$$

where T is the temperature in kelvin. Calculate the wavelength maximum for a blackbody that has been heated to (a) 4000 K, (b) 2000 K, and (c) 1000 K.

7-4 Stefan's law states that the total energy E_T emitted by a blackbody per unit time and per unit area is given by $E_T = \alpha T^4$ where α has a value of 5.69×10^{-8} W M^{-2} K^{-4}. Calculate the total energy output in W/m^2 for each of the blackbodies described in Problem 7-3.

7-5 Relationships described in Problems 7-3 and 7-4 may be of help in solving the following.

(a) Calculate the wavelength of maximum emission of a tungsten filament bulb operated at the usual temperature of 2870 K and at a temperature of 3000 K.

(b) Calculate the total energy output of the bulb in terms of W/cm^2.

7-6 Contrast spontaneous and stimulated emission.

7-7 Describe the advantage of a four-level laser system over a three-level type.

7-8 Define the term *effective bandwidth* of a filter.

7-9 An interference filter is to be constructed for isolation of the CS_2 absorption band at 4.54 μm.

(a) If it is to be based upon first-order interference, what should be the thickness of the dielectric layer (refractive index of 1.34)?

(b) What other wavelengths would be transmitted?

7-10 A 10.0-cm interference wedge is to be built that has a linear dispersion from 400 to 700 nm. Describe details of its construction. Assume that a dielectric with a refractive index of 1.32 is to be employed.

7-11 Why is glass better than fused silica as a prism construction material for a monochromator to be used in the region of 400 to 800 nm?

7-12 For a grating, how many lines per millimeter would be required in order for the first-order diffraction line for $\lambda = 500$ nm to be observed at a reflection angle of 10 deg when the angle of incidence is 60 deg?

7-13 Consider an infrared grating with 72.0 lines per millimeter and 10.0 nm of illuminated area. Calculate the first-order resolution ($\lambda/\Delta\lambda$) of this grating. How far apart (in cm^{-1}) must two lines centered at 1000 cm^{-1} be if they are to be resolved?

7-14 For the grating in Problem 7-13, calculate the wavelengths on the first- and second-order diffraction spectra at reflective angles of (a) 20 deg and (b) 0 deg. Assume the incident angle is 50 deg.

7-15 With the aid of Figures 7-2 and 7-3, suggest instrument components and materials for constructing an instrument that would be well suited for each of the following purposes:

(a) The investigation of the fine structure of absorption bands in the region of 450 to 750 nm.

(b) Obtaining absorption spectra in the far infrared (20 to 50 μm).
(c) A portable device for determining the iron content of natural water based upon the absorption of radiation by the red $Fe(SCN)^{2+}$ complex.
(d) The routine determination of nitrobenzene in air samples based upon its absorption peak at 11.8 μm.
(e) Determining the wavelengths of flame emission lines for metallic elements in the region from 200 to 780 nm.
(f) Spectroscopic studies in the vacuum ultraviolet region.
(g) Spectroscopic studies in the near infrared.

7-16 What is the speed of a lens with a diameter of 4.2 cm and a focal length of 8.2 cm?

7-17 Compare the light-gathering power of the lens described in Problem 7-16 with one that has a diameter of 2.6 cm and a focal length of 8.1 cm.

7-18 A monochromator had a focal length of 1.6 m and a collimating mirror with a diameter of 2.0 cm. The dispersing device was a grating with 1250 lines/mm. For first-order diffraction,
(a) what was the resolving power of the monochromator if a collimated beam illuminated 2.0 cm of the grating?
(b) what is the first- and second-order reciprocal linear dispersion of the monochromator described above?

7-19 A monochromator with a focal length of 0.65 m was equipped with an echellette grating of 2000 blazes per millimeter.
(a) Calculate the reciprocal linear dispersion of the instrument for first-order spectra.
(b) If 3.0 cm of the grating were illuminated, what is the first-order resolving power of the monochromator?
(c) At approximately 560 nm, what minimum wavelength difference could in theory be completely resolved by the instrument?

7-20 Describe the basis for radiation detection with a silicon diode transducer.

7-21 Distinguish among (a) a spectroscope, (b) a spectrograph, and (c) a spectrophotometer.

7-22 A Michelson interferometer had a mirror velocity of 1.25 cm/s. What would be the frequency of the interferogram for (a) UV radiation of 300 nm, (b) visible radiation of 700 nm, (c) infrared radiation of 7.5 μm, and (d) infrared radiation of 20 μm?

7-23 What length of mirror drive in a Michelson interferometer is required to produce a resolution sufficient to separate
(a) infrared peaks at 20.34 and 20.35 μm?
(b) infrared peaks at 2.500 and 2.501 μm?